Internally consistent calibrations for geothermobarometry of high-grade Mg-Al rich rocks in the system MgO-Al_2O_3-SiO_2 and their application to sapphirine-spinel granulites of Eastern Ghats, India and Enderby Land, Antarctica

R K LAL

Department of Geology, Banaras Hindu University, Varanasi 221 005, India

Sixty-three internally consistent geothermobarometers for mineral equilibria involving sapphirine (2 : 2 : 1 and 7 : 9 : 3), pyrope, cordierite, enstatite, Mg-tschermak orthopyroxene, quartz, spinel and sillimanite have been calibrated in the MAS system. The updated thermodynamic data of these minerals are consistent, within limits of error, with high P-T experiments on several mineral equilibria and calorimetric data. The P-T conditions of the granulite facies metamorphism, spanning a range of 700 to more than 1000°C and 4 to more than 10 kbar, can be estimated simultaneously from these geothermobarometers and P-T-t trajectories can be deduced from the reaction coronas well preserved in these rocks because of the refractory nature of aluminous phases.

The geothermobarometers have been applied to sapphirine-spinel granulites of Eastern Ghats and Enderby Land. The P-T conditions of metamorphism (a- prograde/thermal peak and b- retrograde isothermal/isobaric decompression/cooling) estimated for these granulites are: (1) Eastern Ghats (Visakhapatnam): Paderu– (a) 900°C/8.3 kbar, (b-1) 900°C/6.8 kbar and (b-2) 740°C/5.4 kbar; Anantgiri– (a) prograde anticlockwise 930°C/6.2 kbar and (b) 870°C/6.8 kbar, 820°C/6.1 kbar; Anakapalle– (b) 845°C/8.5–6.2 kbar; and Araku– (b) 840°C/6.2 kbar to 795°C/5.9 kbar. Enderby Land (Napier complex): Spot height 945, Tula Mts.– (a) 970°C/9.1 ± 0.6 kbar, isobaric cooling (b) 885°C/7.75 kbar, isothermal decompression (b) 880°C/6.85 kbar; Mt. Hardy, Tula Mts.– (b) 885°C/6.75 kbar; Mt. Riiser-Larsen, Amundsen bay– (a) 1000°C/7.0 kbar prograde anticlockwise; Mt. Sones– (b) 920°C/6.8 kbar; Forefinger Point, SW Enderby Land– (b) 840°C/6.7 kbar, 810°C/6.5 kbar and 775°C/5.0 kbar. The estimated P-T and P-T-t are mostly consistent with those inferred from the granulites of these areas.

1. Introduction

Mg-Al quartz-bearing and quartz-free granulites which are characterized by mineral assemblages containing sapphirine, spinel, sillimanite, cordierite, garnet and hypersthene occur in several localities worldwide. The experimental works in the system MASH* (Schreyer and Seifert 1969; Seifert 1974; Ackermand *et al* 1975; Chatterjee and Schreyer 1972); MAS (Newton 1972); FMASH ± CO_2 (Hensen and Green 1971, 1972, 1973; Bertrand *et al* 1991); and KFMASH (Audibert *et al* 1995; Carrington and Harley 1995a, b) demonstrate that the P-T stability of these granulites ranges from 700° to more than 1000°C and 4 to more than 10 kbar. Most of the univariant and divariant reactions in the MASH and FMASH systems have been inferred from a variety of coronas, symplectites and other reaction textures preserved in these granulites (Caporuscio and Morse 1978; Ellis *et al* 1980; Droop and Bucher-Nurminen 1984; Mohan *et al* 1986; Lal *et al* 1987; Harley *et al*

* Abbreviations and symbols used in this paper are listed at the end of the paper.

Keywords. Geothermobarometry; P-T-t trajectory; sapphirine-spinel granulites; mineral equilibria; calorimetry.

Proc. Indian Acad. Sci. (Earth Planet. Sci.), **106**, No. 3, September 1997, pp. 91–113

1990; Bertrand *et al* 1992 and others) which document signatures of *P-T-t* trajectory of their metamorphic evolution.

The metamorphic conditions of these granulites are inferred from either high *P-T* experiments on mineral equilibria in the MAS, MASH, FMASH and KFMASH systems or from geothermobarometry of the associated granulites. Few attempts have been made till date to calibrate the mineral equilibria involving sapphirine for geothermobarometry of these sapphirine-spinel-bearing granulites based on thermodynamic and calorimetric data in the MAS system (Kleppa and Newton 1975; Droop and Bucher-Nurminen 1984; Waters 1986; Lal 1991; Bertrand *et al* 1992 and Sen *et al* 1995).

Sixty-three out of a total of 71 mineral equilibria in the MAS system involving the minerals mentioned above have potential for geothermobarometry over the entire *P-T* range of granulite facies metamorphism. Only a few mineral equilibria and their existing calibrations for geothermobarometry are applicable to the mineral assemblages of the sapphirine-spinel granulites.

The aim of this paper is: (**a**) to retrieve thermodynamic data of sapphirine (2:2:1 and 7:9:3), spinel, quartz, sillimanite, pyrope, enstatite, Mg-tschermak orthopyroxene and cordierite in the MAS system so that these are consistent with high *P-T* experiments on sapphirine involving and other mineral equilibria as well as calorimetric data of these minerals within the quoted errors; (**b**) to calibrate internally consistent geothermobarometers for sixty three mineral equilibria involving these minerals in the MAS system; and (**c**) to apply these geothermobarometers to estimate the *P-T* and *P-T-t* trajectories of metamorphism of the sapphirine-spinel granulites of the Eastern Ghats and Enderby Land in order to understand the geodynamics and metamorphic evolution of the deep continental crust.

2. Mineral equilibria in the FMAS and MAS systems

In the four components FMAS system there will be a maximum of 21 ($7!/5! \times 2! = 21$) possible univariant reactions between 5 of the 7 minerals (Grt, Crd, Sil, Qz, Spr (7:9:3), Sp and Opx), and 7 invariant points ($7!/6! \times 1! = 7$). Hensen (1986) proposed *P-T* petrogenetic grids for low fO_2 and high fO_2, the former is based on high *P-T* experimental work of Hensen and Green (1971, 1972) in the FMASH system (figure 1A) in which the stable invariant points are [Sp], [Opx], [Sil] and [Qz]. The high fO_2 *P-T* grid (figure 1B), based on inferred reactions and mineral compositions from Spr-Sp granulites displaying evidence of high oxidizing conditions, is characterized by inversion of topology with [Crd], [Grt] and [Spr] as stable invariant points. From each of these invariant points in the low and high fO_2 *P-T* grids, six univariant reactions ($6!/5! \times 1! = 6$) radiate. Similar inversion of topology is possible if Sp contains high contents of Cr_2O_3 or ZnO. In the FMAS *P-T* grid of low fO_2, stable univariant reactions are 18 out of a maximum of 21 (figure 1A), the three metastable univariant reactions are [Spr, Crd], [Grt, Crd] and [Spr, Grt] which are stable in the high fO_2 *P-T* grid (see figure 1B). On the other hand, in the high fO_2 *P-T* grid in the FMAS system (figure 1B) there are 15 stable univariant reactions out of a maximum of 21, and the 6 metastable univariant reactions are [Sil, Sp], [Opx, Sp], [Qz, Sp], [Sil, Opx], [Qz, Opx] and [Qz, Sil] which are stable in the low fO_2 *P-T* grid (see figure 1A). Further, there will be a maximum of 35 ($7!/4! \times 3! = 35$) possible divariant reactions each involving 4 of the 7 minerals. From each univariant reaction involving 5 minerals, 5 divariant reactions ($5!/4! \times 1! = 5$) will emerge (figure 1A, inset bottom left).

With this brief discussion of the FMAS system, we may proceed to the MAS system, involving 8 minerals viz., Pyr, Crd, Sil, Qz, Spr (7:9:3) or Spr (2:2:1), Sp, Ens and MgTs, in which the mineral equilibria have been calibrated in this study for geothermobarometry. Assuming that there are no compositional colinearities between any set of the 3 minerals in the MAS system, the number of univariant reactions each involving 4 minerals out of a maximum of 8 will be 70 ($8!/4! \times 4! = 70$). Out of these 70 univariant reactions there are a maximum of 35 non-degenerate univariant Spr-absent reactions that include 7 minerals ($7!/4! \times 3! = 35$) which are possible in the two sets of reactions involving 8 minerals with Spr (7:9:3) or Spr (2:2:1). Thus the maximum non-degenerate reactions will be 105 ($70 + 70 - 35 = 105$), which reduces to a total of 71 reactions, 60 non-degenerate and 11 degenerate reactions. The degenerate reactions, each involving 3 minerals, are because of compositional colinearity (figure 1A, upper left): (a) Sp, Spr (2:2:1), MgTs, Crd, Qz and (b) Ens, Pyr and MgTs ($5!/3! \times 2! = 10$ and $3!/3! \times 1! = 1$). Out of these 71 reactions, 63 mineral equilibria are potential geothermobarometers which have been calibrated in this study. The 8 mineral equilibria which have been excluded are: Ens + 26Sp + 10Sil = 4Spr(7:9:3), 9Sp + 5Qz = Ens + Spr(7:9:3), 7Sp + 2Sil + Qz = Spr (7:9:3), 5Spr(7:9:3) = Pyr + 12Sil + 32Sp, MgTs + 6Sp + 2Sil = Spr(7:9:3), 2 Sp + Qz = Spr(2:2:1), 5Spr(2:2:1) = Pyr + 2Sil + 7Sp and Ens + 2Sil + 6Sp = 4Spr(2:2:1).

The 63 mineral equilibria calibrated here in the MAS system include 9 minerals [including Spr (7:9:3) and Spr (2:2:1)] mentioned above. The thermodynamic parameters ($\Delta H°f$, $S°$ and $V°$) of these minerals can be retrieved from the high *P-T*

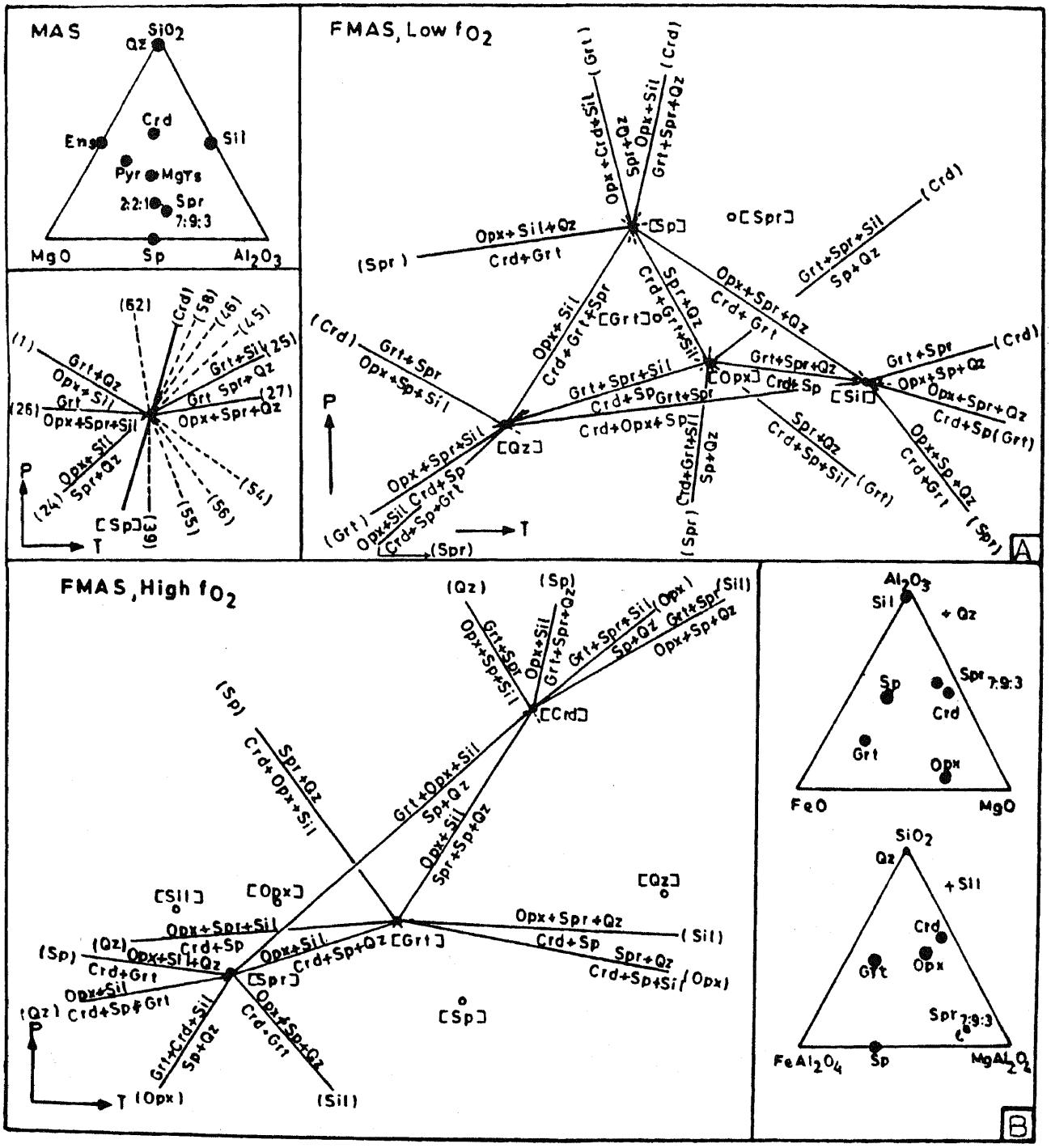

Figure 1. *P-T* petrogenetic grids for low fO_2 (figure 1A) and high fO_2 (figure 1B) in the FMAS system involving sapphirine (7:9:3), spinel, sillimanite, garnet, cordierite, quartz and hypersthene (based on Hensen 1986). Inset in figure 1A: upper left–plot of compositions of the minerals in MgO-Al_2O_3-SiO_2 system (MAS). The mineral equilibria have been calibrated in the MAS system for geothermobarometry in this study. Lower left–schematic *P-T* plot of the (Crd) univariant reaction from [Sp] invariant point in low fO_2 *P-T* petrogenetic grid in FMAS system showing the five divariant mineral equilibria (bold lines). The numbers in parentheses correspond to the equation numbers of the equilibria calibrated in the present study in the MAS system to estimate *P-T* conditions of the (Sp, Crd) mineral assemblage, viz., Opx-Sil-Grt-Spr-Qz. This is an idealized plot in which all the mineral equilibria intersect at a point in the *P-T* diagram. Commonly the mineral equilibria intersect in a field defining a small range of *P-T*. In this and other univariant reactions shown in the low fO_2 and high fO_2 *P-T* petrogenetic grids, five divariant reactions emerge, each of them including four non-degenerate reactions involving Mg-Tschermak orthopyroxene. Inset in figure 1B; upper right relative plots of the compositions of the minerals in the FMAS system in Al_2O_3-FeO-MgO projections from quartz. Lower right–same in SiO_2-$FeAl_2O_4$-$MgAl_2O_4$ diagram, a projection from sillimanite. The reactions shown in the FMAS *P-T* grids of low and high fO_2 can be derived from the relative composition plot of the minerals given in these diagrams.

experimental, calorimetric and published internally consistent datasets. For derivation from high P-T experimental data, linearly independent reactions must be known. Thompson (1982) and Aranovich and Podlesskii (1989) proposed the equation: $n_r = C_p - C_s$, where n_r is the number of linearly independent reactions in the system, C_p is the number of phase components, and C_s is the number of system components. Since $C_p = 9$ and $C_s = 3$ we have $n_r = 6$. Thus if we obtain thermodynamic data of any 6 of the reactions which include all the 9 minerals, these data for other mineral equilibria can be derived by summation of ΔG° of the linearly independent reactions. The 6 linearly independent reactions considered here include equations (1), (2), (12), (9), (39) and (36) given below on which high P-T experimental data are available. Since the experimental data of these equilibria are not tight reversed brackets, both ΔH° and ΔS° of the reactions cannot be retrieved simultaneously. Thus an alternative methodology of stepwise derivation of the thermodynamic data of the minerals from high P-T experiments, calorimetry and published internally consistent datasets has been adopted here.

3. Internally consistent thermodynamic dataset of the minerals used for geothermobarometric calibrations

The thermodynamic parameters, viz., $\Delta H^\circ f_{1000}^{\text{oxide}}$, S°_{1000} and $V^\circ_{7,1000}$ of Spr(2:2:1 and 7:9:3), Pyr, Crd, Ens, MgTs, Qz, Sp and Sil retrieved or obtained from other sources, are given in table 1.

The volumes ($V^\circ_{7,1000}$ cm^3 mol^{-1}) of all the minerals, except Spr, are taken from the internally consistent thermodynamic dataset of Holland and Powell (1990). The molar volumes ($V^\circ_{1,1000}$) of $Spr_{2:2:1}$ and $Spr_{7:9:3}$ are from Kleppa and Newton (1975) and Waters (1986) respectively, which have been calculated from $V^\circ_{1,298}$ of these end members of sapphirine by assuming isobaric thermal expansion coefficient of spinel. The coefficient of isothermal compressibility of spinel given in Holland and Powell (1990) has been used to calculate their $V^\circ_{7,1000}$ cm^3 mol^{-1} (the difference in $V^\circ_{7,1000}$ is ± 1 cm^3 mol^{-1} only if the compressibility terms of enstatite or diopside or wollastonite are taken).

The $\Delta H^\circ f_{1000}^{\text{oxide}}$ and S°_{1000} (henceforth abbreviated $\Delta H^\circ f$ and S°) of sillimanite are from Robie *et al* (1978) and S° of quartz is from Berman (1988). For enstatite, $\Delta H^\circ f$ and S° are taken from Clemens *et al* (1987; and references given therein) and Newton and Perkins (1982) respectively which are based on calorimetry. The S° of other minerals are also mostly from calorimetry, e.g., pyrope (Newton and Perkins 1982), $sapphirine_{2:2:1}$ (Kleppa and Newton 1975, calculated by oxide summation), cordierite (Robie *et al* 1978) which includes configurational entropy of 1.48 cal K^{-1} mol^{-1}, spinel (Robie *et al* 1978) including configurational entropy of 1.58 cal K^{-1} mol^{-1} (Newton 1987). Using these thermodynamic parameters as knowns, the $\Delta H^\circ f$ of $sapphirine_{2:2:1}$, cordierite, spinel and pyrope have been derived from the reversed experimental data on the linearly independent mineral equilibria.

For $sapphirine_{2:2:1}$, $\Delta H^\circ f$ has been retrieved from high P-T experiments on the reaction

$$\text{Ens} + 2\text{Sil} = \text{Spr}_{2:2:1} + 3\text{Qz} \ldots (\text{Sp, Crd, Pyr})$$

of Chatterjee and Schreyer (1972) and Newton (1972), with input of known $\Delta H^\circ f$ of enstatite and sillimanite from the equation:

$$\Delta H^\circ f\ \text{Spr}_{2:2:1} = \Delta H^\circ f\ \text{Ens} + 2\Delta H^\circ f\ \text{Sil} - \Delta H^\circ f \text{ reaction (Sp, Crd, Pyr).}$$

Table 1. *Thermodynamic data of minerals.*

Minerals	Composition	$\Delta H^\circ f_{1000}^{\text{oxide}}$ kcal mol^{-1}	S°_{1000} cal K^{-1} mol^{-1}	$V^\circ_{7,1000}$ cms mol^{-1}
Pyrope (Pyr)	$Mg_3Al_2Si_3O_{12}$	−19.48	185.83	115.05
Sillimanite (Sil)	Al_2SiO_5	−0.52	70.52	50.43
$Sapphirine_{2:2:1}$ ($Spr_{2:2:1}$)	$Mg_2Al_4SiO_{10}$	−10.41	158.75	100.46
$Sapphirine_{7:9:3}$ ($Spr_{7:9:3}$)	$Mg_7Al_{18}Si_3O_{40}$	−36.72	630.26	400.00
Spinel (Sp)	$MgAl_2O_4$	−5.70	64.79	40.44
Enstatite (Ens)	$Mg_2Si_2O_6$	−16.72	93.51	63.72
Cordierite (Crd)	$Mg_3Al_4Si_5O_{18}$	−16.54	270.73	232.84
β Quartz (Qz)	SiO_2	0.00	27.78	23.58
Mg-tschermak Orthopyroxene (MgTs)	$MgAl_2SiO_6$	−0.20	94.20	59.94

The thermodynamic data of these minerals have been retrieved in this study or obtained from other sources. See section 3 of the text. The error in the thermodynamic parameters of the minerals except $Spr_{7:9:3}$ are the same as given in Robie *et al* (1978), Holland and Powell (1990), Charlu *et al* (1975) and other workers, see also section 3 of the text.

The $\Delta H°f$ of sapphirine$_{2:2:1}$ is -10.41 kcal mol^{-1} which is in agreement with -10.24 ± 0.3 kcal mol^{-1} obtained from calorimetry by Kleppa and Newton (1975). The P-T curve, using the thermodynamic data of the minerals involved in the (Sp, Crd, Pyr) reaction passes through all the experimental brackets (figure 2A). The pronounced change in dP/dT slope of the reaction is due to an increase in alumina solubility in enstatite with increase in temperature. Following the same procedure as given for derivation of $\Delta H°f$ of sapphirine$_{2:2:1}$, $\Delta H°f$ of cordierite is obtained from the experimental data (Newton 1972) of the degenerate reaction in the MAS system $Spr_{2:2:1} + 4Qz = Crd$..... (Sil, Ens, Sp, Pyr) for the breakdown of anhydrous cordierite using the known input of $\Delta H°f$ of $Spr_{2:2:1}$ retrieved from the (Sp, Crd, Pyr) reaction. The $\Delta H°f$ of cordierite derived is -16.54 kcal mole^{-1} which is consistent with -16.28 ± 0.48 kcal mol^{-1} obtained from calorimetry by Charlu *et al* (1975). The P-T curve plotted, using the thermodynamic data of the minerals of the reaction (Sil, Ens, Sp, Pyr), passes through the experimental brackets (figure 2A) of Newton (1972). As a cross check, the plot of the P-T curve of the reaction

$$Ens + 2Sil + Qz = Crd..... \text{ (Spr, Sp, Pyr)}$$

for which the thermodynamic data of all the minerals are now known, is consistent with those derived from the 'THERMOCALC' computer programme of Holland and Powell (1990) (figure 3A). Similarly, $\Delta H°f$ of pyrope has been derived from the experimental data of the reaction

$$2Pyr + 3Qz = 3Ens + 2Sil..... \text{ (Crd, Spr, Sp)}$$

of Perkins (1983) in the MAS system (figure 2B). The derived value of $\Delta H°f$ pyrope is -19.48 kcal mol^{-1} and is slightly less negative compared to -20.21 ± 0.5 kcal mol^{-1} obtained from calorimetry by Charlu *et al* (1975). The high P-T experimental data on the reaction $Grt + Sil + Qz = Crd$ in the FMASH ($\pm CO_2$) under the condition P_{H_2O} ($\pm CO_2$) = P_{Total} have been plotted in the $P_{Experimental}$ vs $P_{Estimated}$ diagram (figure 2F). $P_{Estimated}$ is obtained from the thermodynamic data of the minerals of the reaction

$$2Pyr + 4Sil + 5Qz = 3Crd..... \text{ (Ens, Spr, Sp)}$$

with a correction for the hydration state of cordierite (equation is given in figure 2) and assuming ideal Fe-Mg mixing in Grt and Crd. The estimated P at given T is consistent with those of the experiments. Figure 2I is a similar plot of Grt-Sil-Qz-Crd equilibrium from experiments on dehydration (or fluid absent) melting in the KFMASH system (Carrington and Harley 1995b) where $P_{Estimated}$ is from (Ens, Spr, Sp) reaction for the conditions $P_{H_2O} = 0$, $P_{H_2O} = P_{Total}$ and $P_{H_2O} = 0.5P_{Total}$. The data plotting on the $P_{Experimental} = P_{Estimated}$ line suggest the condition between $P_{H_2O} = 0$ and $P_{H_2O} = 0.5P_{Total}$ in the experiments, in agreement with Carrington and Harley (1995b) who have proposed that cordierite is undersaturated in H_2O compared to the coexisting melt phase.

The P-T curves of the reactions involving Ens, Sil, Crd, Pyr and Qz derived from the thermodynamic data given above are compared with those from the 'THERMOCALC' and 'TWQ' (June, 1992) programmes of Holland and Powell (1990) and Berman (1988) respectively (figures 3A to 3E).

The $\Delta H°f$ of spinel (-5.70 kcal mol^{-1}) has been extracted from the experimental data in the ZnFMASH system of the reaction

$$Grt + Sil = Sp_{ss} + Qz$$

of Nichols *et al* (1992) assuming ideal mixing of Fe-Mg in garnet and spinel and non-ideal Fe-Zn and Mg-Zn mixing in spinel given in Nichols *et al* (1992). The calculated pressures for the temperature range 850–1100°C from their experiments are in reasonable agreement (figure 2E). The derived $\Delta H°f$ of spinel is in agreement with the value of -5.38 ± 0.5 kcal mol^{-1} of spinel obtained from calorimetry by Charlu *et al* (1975). The plot of the P-T curve of the metastable reaction

$$Pyr + 2Sil = 3Sp + 5Qz..... \text{ (Spr, Crd, Ens)}$$

in the MAS system derived from the thermodynamic data of the minerals given above is shown in figure 2D and compared with those of Nichols *et al* (1992) and 'TWQ' and 'THERMOCALC' programmes of Berman (1988) and Holland and Powell (1990) respectively. The P-T curves of the reactions from the 'TWQ' and 'THERMOCALC' differ considerably from those of the present study. The application of these computer programs to estimate P-T conditions of metamorphism of granulites containing Sp-Qz-Grt-Sil assemblage would require very high and unrealistic negative deviation of non-ideal mixing of Fe-Mg in spinel. This is depicted in figures 4H and 4I which show the P-T curves of the reactions from the experimental run products of the sample no. T 3190 at 1050 ± 10°C and 12 ± 0.5 kbar of the equilibrium assemblage containing Grt, Sp, Opx, Sil and Qz in the ZnFMAS system (Nichols *et al* 1992). The P-T derived from the intersection of the reaction curves

$$2Pyr + 3Qz = 3Ens + 2Sil..... \text{ (Sp) and}$$

$$Pyr + 2Sil = 3Sp + 5Qz..... \text{ (Ens),}$$

using the 'TWQ' of Berman (1988) are 1390°C/9.6 kbar which is inconsistent with those of the experiments (figure 4H). In the calculation of the activities of Pyr, Sp and Opx, non-ideal subregular solution for Fe-Mg mixing (Berman and Koziol 1991), regular solution for Zn-Fe-Mg mixing (Nichols *et al* 1992) and two site mixing (Wood and Banno 1973) have been used respectively. Figure 4I

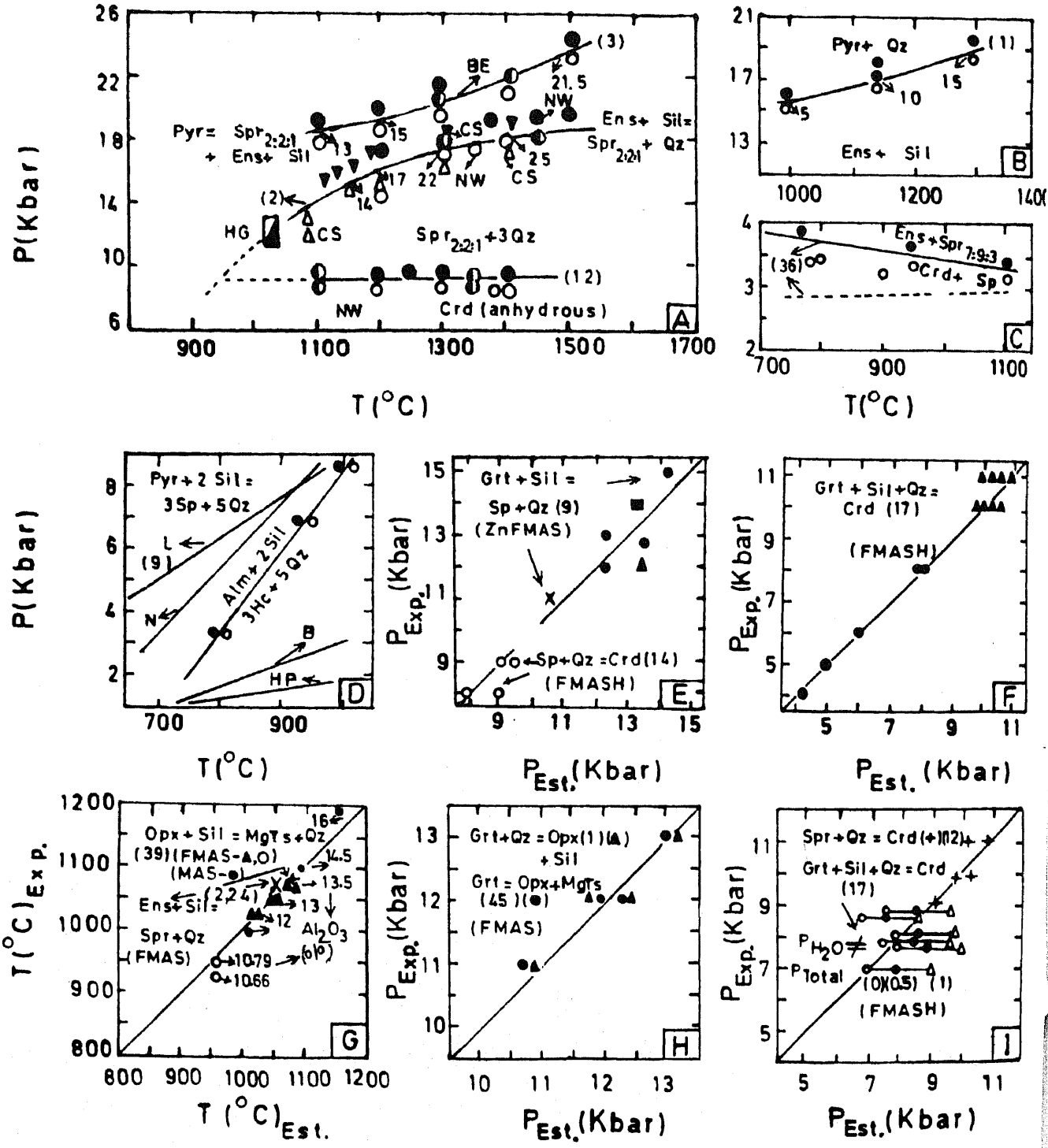

Figure 2. (A), (B) and (C) = P-T plots of the experimental data in the MAS system of the reactions (2), (3) and (12) in (A), (1) in (B) and (36) in (C). Reaction (12) involves anhydrous Crd. Filled symbols–reactants stable, open symbols–products stable and half filled symbols–no reaction observed. The curves passing through the experimental brackets of the reactions given in the figures are derived from the corresponding equations viz., (2), (3), (12), (1) and (36) of the geothermobarometers of the present study given in the text. CS–Chatterjee and Schreyer (1972), NW–Newton (1972), HG–Hensen and Green (1971), BE–Boyd and England (1959) in (A); (B) Perkins (1983) and (C) Seifert (1974) in the MASH system. In the reaction curves shown for the Ens-bearing equilibria (2), (3) and (1), the Al_2O_3-contents (wt%) of Ens (numbers without parentheses) given by the respective authors are considered for calculating X_{Ens}. For the reaction (2) Al_2O_3-contents of Ens are from CS. Besides this, in Crd-bearing equilibrium (36) shown in (C), hydration state of Crd has been included, besides the Al_2O_3-contents of Ens. In (C) the calculated curve for the reaction (36) from equation (36) of this study, for $X_{H_2O} = 0$ and activity of all the mineral equal to 1, is also shown by dashed line. For hydrous cordierite-bearing equilibria pressure at given temperature has been estimated from the equation $P = 1 + \{[T(\Delta S^\circ - R\ln K) - \Delta H^\circ + n(2414 - 1.95525T)]/(\Delta V^\circ - n\ 0.2457)\}$ for the condition $P_{H_2O} = P_{Total}$, modified after Aranovich and Podlesskii (1989). n = number of moles of Crd in the reactions. For the condition $P_{H_2O} = 0.5$ or $0.25\ P_{Total}$, the numerator and denominator of the hydration equation of cordierite $n(2414 - 1.95525T)/-\ n\ 0.2457$ have to be multiplied by 0.5

shows a similar plot from 'THERMOCALC' of Holland and Powell (1990) in which Fe-Mg mixing in Grt and Sp is assumed to be ideal, activity of Sp is calculated from non-ideal mixing of Zn-Fe and Zn-Mg of Nichols *et al* (1992) and X_{Ens} from Wood and Banno (1973). The *P-T* corresponding to those of the experiments are matched only if γ_{Sp} is assumed to be 0.656 in the 'TWQ' and 0.625 in the 'THERMOCALC'. Further the K_D of the (Spr, Crd, Ens) reaction derived from experiments (Nichols *et al* 1992) and these granulites is approximately 1.0 ± 0.2. Thus the *P-T* curve of this reaction should lie close to those of the reaction

Almandine + 2Sillimanite = 3Hercynite + 5Quartz

in the FAS system experimentally reversed with tight brackets by Bohlen *et al* (1986) as shown in figure 2D. This suggests that the *P-T* curve of the reaction (Spr, Crd, Ens) from this study is reasonable. The *P-T* plots of other mineral equilibria involving spinel from this study and their comparison with those derived from 'TWQ' and 'THERMOCALC' are depicted in figures 3F to 3I and figures 3K and 3L. The salient features apparent from these plots are: (**a**) The *P-T* plots of the quartz-absent spinel-cordierite equilibria, viz., 5Ens + 10Sil = 4Crd + 2Sp..... (Qz, Spr, Pyr) and

Pyr + 2Sil = Sp + Crd..... (Ens, Qz, Spr)

from this study agree with the 'TWQ' and 'THERMOCALC' (figures 3F and 3G) because of high ΔV° of the reactions. (**b**) There is considerable discrepancy in the *P-T* plots of the reactions

4Pyr = 5Ens + 2Sil + 2Sp..... (Spr, Qz, Crd),

Pyr = Ens + Sp + Qz..... (Spr, Sil, Crd),

Ens + 2Sil = 2Sp + 4Qz..... (Spr, Pyr, Crd)

(figures 3H, 3K and 3L). (**c**) $\Delta H^\circ f$ and S° for spinel in 'TWQ' and 'THERMOCALC' have been mostly retrieved from experimental work at 700–750°C on dehydration reactions involving chlorite which have high ΔH° and ΔS°. In order to apply anhydrous spinel-quartz ± pyrope equilibria, lacking cordierite, to estimate *P-T* conditions of metamorphism in the granulite facies, it is desirable that the thermodynamic parameters of spinel given in 'TWQ' and 'THERMOCALC' are revised. This problem can only be resolved by further experiments on these anhydrous equilibria in the FMAS system at low fO_2.

The $\Delta H^\circ f$ and S° of sapphirine$_{7:9:3}$ have been derived from the reversed experimental data of the reaction

Ens + $Spr_{7:9:3}$ = Crd + 7Sp..... (Qz, Sil, Pyr)

of Seifert (1974) in the MASH system. A graphical plot of (P-1)ΔV° + RTlnK vs $T(K)$ yields a slope ΔS° and intercept at ^{0}(K) of $-\Delta H^\circ f$ of the reaction. The equilibrium constant (K) includes reduced activity of enstatite due to alumina solubility and of cordierite due to its hydration state. With the input of derived thermodynamic parameters $\Delta H^\circ f$ and ΔS° of the reaction and the $\Delta H^\circ f$ and S° of enstatite, cordierite and spinel, the unknown $\Delta H^\circ f$ and S° of sapphirine$_{7:9:3}$ have been derived. The *P-T* curves of the end member reaction in the MAS system involving anhydrous cordierite and the Al-free

---

Figure 2 caption continued

or 0.25. The equation is also applicable if the fluid phase is mixture of H_2O and CO_2 or CO_2 as the increase in pressure of stability of H_2O or CO_2-bearing cordierite involving equilibria relative to anhydrous cordierite is nearly the same (cf. Bertrand *et al* 1991). $X_{Ens} = 1.00059 - 0.019847$ wt% Al_2O_3 in Ens (applicable to the MAS and MASH systems only).

(**D**)–The curve of the metastable end-member reaction (9) calculated from the equation (9) of the present study is compared with those of 'Twq' (Berman 1988-B), "THERMOCALC" (Holland and Powell 1990-HP) and Nichols *et al* (1992-N). The end member reaction Alm + 2Sil = 3Hc + 5Qz experimentally studied by Bohlen *et al* (1986) is also shown. Hc-hercynite, Alm-almandine. See text for discussion.

(**E**), (**F**), (**G**), (**H**) and (**I**) = Plots of $P_{experimental}$ vs $P_{estimated}$ and $T_{experimental}$ vs $T_{estimated}$ of the different mineral equilibria in the systems mentioned in the figures. Numbers within parentheses are the equation numbers of the calibrations of the present study. The line P or $T_{experimental} = P$ or $T_{estimated}$ are also shown. For Crd with $H_2O \pm CO_2$ the equation given above has been used to calculate pressures at given temperatures along with the present calibration of anhydrous cordierite involving mineral equilibria. Sources of experimental data in the figures are as follows: (E) Equation (9)- Nichols *et al* (1992) filled square–1100°C, filled circle–1050°C, filled triangle–950°C and cross–850°C. Equation (14) Bertrand *et al* (1991), *P-T* range 8–9 kbar and 1025–1050°C. (F) Equation (17)–Filled circle–Aranovich and Podlesskii (1983) in the range of 700–750°C, and filled triangle–Bertrand *et al* (1991) in the range 900–1050°C (fluid composition $H_2O \pm CO_2$). (G) Equation (39)–Filled triangle-Bertrand *et al* (1991), in *P-T* range 11–13 kbar and 1025–1075°C. Open circles–Carrington and Harley (1995b), run numbers DG55-17 and DS 45-15 at 950°C/8.5 kbar and 925°C/12.5 kbar respectively. Filled circle–Hensen and Essene (1971), 1000°C/15.3 kbar 1100°C/14.4 kbar and 1200°C/15.3 kbar. Al_2O_3 contents in orthopyroxene are in wt% except those of Bertrand *et al* (1991) which are in mole%. The maximum Al_2O_3 contents determined by them at 1025 and 1075°C are 14 mole% which has been assumed to be 12 and 13.5 mole% respectively, so that these are consistent with their experimental data at 1050°C where maximum Al_2O_3 in orthopyroxene is 13 mole%. Equations (2) and (24)–Bertrand *et al* (1991) in FMAS system, small and larger crosses are equations (2) and (24) involving $Spr_{2:2:1}$ and $Spr_{7:9:3}$ respectively, *P-T* 1075°C/12 kbar. (H) Equations (1) and (45)–Bertrand *et al* (1991) in *P-T* range 11–13 kbar and 1025–1075°C. (I) Equation (12)–Bertrand *et al* (1991) in the *P-T* range 10–11 kbar and 1050–1300°C. Equation (17)–dehydration melting in the KFMASH system (Carrington and Harley 1995b) in *P-T* range 7–8.75 kbar and 873–910°C; Open circle, solid circle and open triangle represent $P_{H_2O} = 0, 0.5$ and 1.0 P_{Total} respectively. See equation for hydrous cordierite given above.

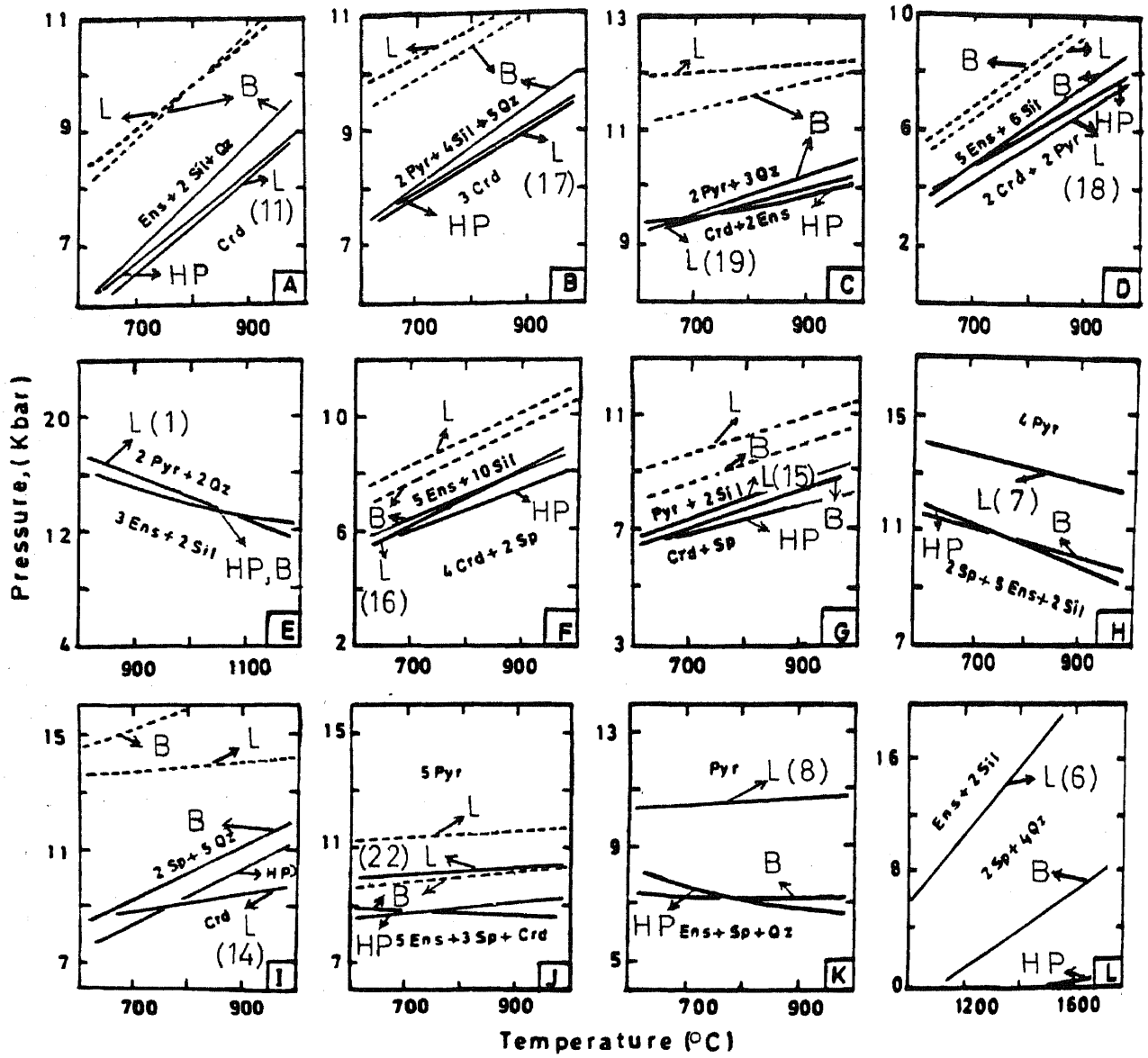

Figure 3. In (**A**), (**B**), (**C**), (**D**) and (**E**) the different end member equilibria (solid curves) involving Ens, Sil, Pyr, Qz and Crd (dry) derived from the equation numbers given in parentheses of the present calibrations for geobarometry (L) are compared with those of 'TWQ' (B) and 'THERMOCALC' (HP). (**F**), (**G**), (**H**), (**I**), (**J**), (**K**) and (**L**)–same as above for the different mineral equilibria involving Ens, Sil, Crd (dry), Sp, Qz and Pyr. The dashed lines show the P-T positions of Crd involving reactions under the condition $P_{H_2O} = P_{Total}$ calculated from the above mentioned equations in which Crd is anhydrous along with the equation of hydration of Crd given in figure 2. Similar plots from 'TWQ' (B) are also shown for comparison.

enstatite calculated from the thermodynamic data of minerals from this study, and under the condition $P_{H_2O} = P_{Total}$, including the RTlnK term which passes through all the experimental brackets of the reaction given in Seifert (1974), are shown in figure 2C. Using the thermodynamic data of sapphirine$_{7:9:3}$, the P-T curves of the different dehydration reactions involving sapphirine$_{7:9:3}$, clinochlore, enstatite, corundum and cordierite have been calculated with minor adjustment of $\Delta H°f$ of clinochlore given in Berman (1988) and Holland and Powell (1990), and $V°$ and $S°$ of corundum from Robie *et al* (1978). These reaction curves pass through all the reversed brackets determined experimentally by Seifert (1974) in the MASH system under the condition $P_{H_2O} = P_{Total}$. The retrieved $\Delta H°f$ and $S°$ of sapphirine$_{7:9:3}$ of -36.72 kcal mol^{-1} and 630.26 cal K^{-1} mol^{-1} respectively differ significantly from those given in Waters (1986), although derived from the (Qz, Sil, Pyr) reaction of Seifert (1974), because Waters (1986) has used the thermodynamic dataset of all other minerals given in Harris and Holland (1984).

The $\Delta H°f$ and $S°$ of Mg-tschermak orthopyroxene are derived from the experimental data of mineral equilibria involving orthopyroxene, sillimanite, quartz and cordierite in the MASH and FMASH systems of Aranovich and Podlesskii (1989 and references given therein) assuming two site ideal mixing in

orthopyroxene given by Wood and Banno (1973) and their calibration of the reaction

$$AlAlO_3 \text{ (Fictive Al} - \text{orthopyroxene)} + Qz = Sil$$

based on these experiments. The retrieved $\Delta H°f$ of Mg-tschermak orthopyroxene $-0.20\,kcal\,mol^{-1}$ is within the range -0.09 (Holland and Powell 1990), -1.14 (Gasparik and Newton 1984) and $+0.40$ (Newton 1987) $kcal\,mol^{-1}$; $S°$ ($cal\,K^{-1}\,mol^{-1}$) of 94.0 is higher in comparison to 92.02 (Holland and Powell 1990) and 93.51 (Newton 1987). Apart from the present study, the thermodynamic parameters of Mg-tschermak orthopyroxene have been generally derived from experiments on alumina contents of orthopyroxene coexisting with either pyrope or pyrope-spinel-forsterite. Figure 2G shows the experimental data of the reaction Opx + Sil = MgTs + Qz in FMAS and MAS systems in $T_{Experimental}$ vs $T_{Estimated}$ diagram where $T_{Estimated}$ is from the reaction

$$Ens + 2Sil = 2MgTs + 2Qz \ldots\ldots \text{ (Pyr, Crd, Spr, Sp)}.$$

The plots are close to the line $T_{Experimental} = T_{Estimated}$ suggesting that the thermodynamic data of MgTs are reasonable.

We have the thermodynamic data of the 9 minerals from the 6 linearly independent reactions now. Thus all other mineral equilibria can be calibrated from this internally consistent thermodynamic dataset. The plots of P or $T_{Experimental}$ vs P or $T_{Estimated}$ of other mineral equilibria, for which few experimental data are available, are depicted in figures 2E, 2G, 2H and 2I. These further suggest that the thermodynamic data retrieved or obtained from other sources are reasonably good.

The thermodynamic data of the minerals (table 1) have been used to calibrate sixtythree mineral equilibria for geothermobarometry in MAS system.

4. Internally consistent calibrations of the geothermobarometers

A simplified thermodynamic expression has been used for the calibrations because reliable heat capacity

Table 2a. *Electron microprobe analyses of minerals from Spr-Sp granulites of Paderu, Eastern Ghats used for geothermobarometry.*

Sample no.	H-1						321				
	Grt^C	Grt^R	Opx^C	Opx^R	Spr	Sp	$Grt^{C,R}$	Opx^C	Opx^R	Spr	Sp
SiO_2	40.79	40.51	48.06	49.01	11.88	—	38.83	47.31	49.33	12.16	—
TiO_2	0.02	0.02	0.11	0.10	0.02	—	—	—	0.27	—	—
Al_2O_3	22.46	22.53	9.28	7.98	63.39	62.69	22.29	9.75	7.86	61.48	60.22
Cr_2O_3	—	0.02	—	—	0.09	0.44	—	—	—	0.39	1.42
*FeO	23.95	23.93	20.62	20.43	10.40	24.92	23.59	19.78	19.02	10.55	23.34
MnO	0.42	0.39	0.09	0.09	—	0.05	0.62	0.23	0.38	—	0.29
MgO	12.69	12.58	21.12	21.62	14.42	12.34	13.25	21.55	22.61	15.34	12.82
CaO	0.21	0.23	—	—	—	—	0.23	—	—	—	—
ZnO	—	—	—	—	—	—	—	—	—	—	0.80
Total	100.54	100.21	99.28	99.23	100.20	100.44	98.81	98.62	99.47	99.92	100.88
O	24	24	6	6	20	8	24	6	6	20	8
Si	6.087	6.067	1.783	1.817	1.423	—	5.924	1.758	1.815	1.460	—
Ti	0.002	0.002	0.003	0.003	0.002	—	—	—	0.007	—	—
Al	3.950	3.978	0.405	0.349	8.951	3.907	4.008	0.427	0.341	8.701	3.761
Cr	—	0.002	—	—	0.009	0.018	—	—	—	0.037	0.059
Fe^{3+}	—	—	0.023	0.011	0.190	0.075	—	0.057	0.014	0.341	0.180
Fe^{2+}	2.988	2.997	0.616	0.622	0.852	1.026	3.009	0.558	0.571	0.719	0.942
Mn	0.053	0.049	0.003	0.003	—	—	0.080	0.007	0.012	—	0.013
Mg	2.822	2.808	1.167	1.195	2.574	0.972	3.012	1.193	1.240	2.744	1.013
Ca	0.034	0.037	—	—	—	—	0.038	—	—	—	—
Zn	—	—	—	—	—	—	—	—	—	—	0.032
X_{Mg}	0.486	0.484	0.655	0.658	0.751	0.486	0.500	0.681	0.685	0.792	0.518

$X_{Mg} = Mg/(Mg + Fe^{2+})$. *Total iron as FeO. C-core, R-rim/corona. Spr and Sp are in contact with quartz, Core and rim compositions of Grt and Opx used for estimating P-T of the thermal peak and coronas respectively.
Mineral present: Grt-Spr-Sp-Opx-Qz-Kf-Sil (Ilmenite-hematite intergrowth, Rutile)

The Fe^{3+} contents of Opx, Sp and Spr(2:2:1 and 7:9:3) are calculated from stoichiometry after normalizing the formula to 4, 6 and 14 cations respectively (cf. Lal *et al* 1984 and Mohan *et al* 1986 and references given therein): Opx: $Fe^{3+} = Al^{IV}$-(Al^{VI} + Cr + 2Ti-Na), Al^{IV} = 2-Si, and Al^{VI} = total Al-Al^{IV} based on formula normalized to 4 cations.

Sp: Fe^{3+} = 16-($2R^{+2}$ + 4Ti + $3R^{3+}$ cations).

Spr(2:2:1 and 7:9:3): $Fe^{3+} = Al^{IV}$-(Al^{VI} + Cr + 2Ti), Al^{IV} = 6-Si, and Al^{VI} = total Al-Al^{IV} based on formula normalized to 14 cations.

Table 2b.

Sample no.	17 II				259				
	Opx^C	Opx^R	Spr	Crd	Grt^C	Grt^R	Opx^C	Opx^R	Crd
SiO_2	49.32	49.91	13.07	50.29	40.34	39.54	49.60	49.95	48.05
TiO_2	0.08	0.08	—	—	—	—	0.24	0.23	—
Al_2O_3	9.55	8.59	63.03	33.35	22.71	22.52	9.64	8.44	32.98
Cr_2O_3	—	—	—	—	—	—	—	0.10	—
*FeO	16.60	16.78	7.89	2.75	22.70	22.82	17.09	18.15	3.91
MnO	0.10	0.14	0.05	0.03	1.02	0.96	—	0.39	0.18
MgO	24.17	24.64	16.38	11.82	13.78	13.29	23.60	23.00	11.88
CaO	0.05	—	—	—	0.74	0.75	—	—	—
Total	99.87	100.14	100.42	98.24	101.21	99.90	100.17	100.26	97.00
O	6	6	20	18	24	24	6	6	18
Si	1.782	1.798	1.545	5.043	5.976	5.853	1.792	1.815	4.927
Ti	0.002	0.002	—	—	—	—	0.006	0.006	—
Al	0.407	0.365	8.781	3.942	3.966	3.996	0.411	0.362	3.986
Cr	—	—	—	—	—	—	—	0.003	—
Fe^{3+}	0.025	0.036	0.129	—	—	—	—	—	—
Fe^{2+}	0.477	0.469	0.659	0.234	2.812	2.872	0.516	0.522	0.335
Mn	0.003	0.004	0.005	0.002	0.128	0.125	—	0.012	0.016
Mg	1.301	1.323	2.885	1.766	3.042	2.981	1.271	1.246	1.815
Ca	0.002	—	—	—	0.117	0.121	—	—	—
X_{Mg}	0.732	0.738	0.814	0.883	0.520	0.509	0.711	0.693	0.844

Mineral present: Opx-Sil-Spr-Crd-Qz-Kf (Biotite, Rutile).

Spr is not in contact of Qz, and is rimmed partially by Opx, Sil and Crd in coronas–17II.

Grt-Opx-Sil-Crd-Qz-Kf (Biotite, Rutile)–259.

Table 2c.

Sample no.	244							
	Grt1	Opx1	Crd1	Spr1	Sp1	Grt2	Spr2	Sp2
SiO_2	39.57	50.22	52.23	12.74	—	38.71	12.38	—
TiO_2	—	—	—	—	1.04	—	—	—
Al_2O_3	22.33	7.74	32.35	62.50	61.50	22.09	62.14	60.63
Cr_2O_3	—	—	—	—	1.50	—	0.62	1.96
*FeO	23.07	18.35	2.45	8.08	20.02	22.15	8.30	21.33
MnO	0.60	—	—	—	—	0.68	—	0.22
MgO	13.70	23.20	11.01	16.18	14.46	14.33	16.06	14.35
CaO	0.22	—	—	—	—	0.22	—	—
ZnO	—	—	—	—	1.50	—	—	0.53
Total	99.49	99.51	98.04	99.50	100.12	98.18	99.50	99.02
O	24	6	18	20	8	24	20	8
Si	5.970	1.837	5.220	1.521	—	5.911	1.482	—
Ti	—	—	—	—	0.041	—	—	—
Al	3.971	0.334	3.811	8.795	3.818	3.976	8.766	3.800
Cr	—	—	—	—	0.063	—	0.059	0.082
Fe^{3+}	—	—	—	0.163	0.037	—	0.212	0.118
Fe^{2+}	2.910	0.561	0.205	0.643	0.844	2.828	0.618	0.830
Mn	0.077	—	—	—	0.004	0.088	—	0.010
Mg	3.080	1.264	1.640	2.878	1.135	3.261	2.864	1.137
Ca	0.036	—	—	—	—	0.036	—	—
Zn	—	—	—	—	0.058	—	—	0.023
X_{Mg}	0.514	0.693	0.889	0.817	0.573	0.536	0.823	0.578

Minerals present: Grt-Opx-Sil-Spr-Sp-Crd-Qz-Kf (Biotite, Rutile). Sp and Spr are not in contact of Qz and Crd. Spr1-Sp1-Opx1-Grt1 are from corona with Sp1-Spr1 which are successively rimmed by Sil, Opxl and Grt1; Grt2, Spr2 and Sp2 are from coronas (with core to rim of coronas): Sp-Sa-Grt-Qz, Sp-Sa-Sil-Grt, Sp-Sil-Grt-Qz, Sa-Sil-Grt-Qz.

Table 2d.

Sample no.	252				258		
	Grt^R	Sp	Opx^R	Crd	Sp	Opx	Crd
SiO_2	38.14	—	48.47	47.51	—	47.75	47.63
TiO_2	—	—	—	—	—	—	—
Al_2O_3	22.33	59.15	5.35	33.04	60.37	6.80	32.53
Cr_2O_3	—	—	—	—	—	—	—
*FeO	27.91	31.45	25.95	5.48	29.60	25.49	5.14
MnO	1.07	0.68	0.68	0.24	0.50	0.60	—
MgO	10.09	7.62	17.79	11.60	9.67	18.85	12.21
CaO	0.85	—	—	—	—	—	—
ZnO	—	1.00	—	—	—	—	—
Total	100.39	99.90	98.24	97.87	100.14	99.49	97.51
O	24	8	6	18	8	6	18
Si	5.870	—	1.873	4.873	—	1.808	4.892
Ti	—	—	—	—	—	—	—
Al	4.051	3.849	0.243	3.994	3.855	0.303	3.983
Cr	—	—	—	—	—	—	—
Fe^{3+}	—	0.151	0.011	—	0.145	0.081	—
Fe^{2+}	3.591	1.300	0.827	0.470	1.196	0.725	0.441
Mn	0.139	0.032	0.022	0.021	0.023	0.019	—
Mg	2.314	0.627	1.024	1.773	0.781	1.063	1.868
Ca	0.140	—	—	—	—	—	—
Zn	—	0.041	—	—	—	—	—
X_{Mg}	0.392	0.325	0.553	0.790	0.395	0.595	0.809

Minerals present: Grt-Sp-Opx-Crd-Sil-Qz-Plag-(An29.8)-Kf-(Biotite, Ilmenite-hematite intergrowth). Coronas-Sp is successively rimmed by Sil and Opx, and Sp with a rim of Crd–252.
Sp-Opx-Crd-Sil-Qz-Kf (Biotite, Ilmenite-hematite intergrowth). Coronas: Sp successively rimmed by Sil and Opx, and Sp with rim of Crd–258.

(C_p^0) data from calorimetry for sapphirine and Mg-tschermak orthopyroxene are not available

$$\Delta G_{P,T}(\text{reaction}) = 0 = \Delta H^\circ_{1000} - T\Delta S^\circ_{1000} + (P-1)\Delta V^\circ_{7,1000} + \text{nRTlnK} \quad \text{(A)}$$

The equation (A) is rearranged for the formulation of geothermometers (equation B) and geobarometers (equation C)

$$T(K) = \{[(P-1)\Delta V^\circ_{7,1000} + \Delta H^\circ_{1000}]/(\Delta S^\circ_{1000} - R\ln K)\} \quad \text{(B)}$$

$$P(\text{bars}) = 1 + \{[T(\Delta S^\circ_{1000} - R\ln K) - \Delta H^\circ_{1000}]/\Delta V^\circ_{7,1000}\} \quad \text{(C)}$$

The abbreviation and symbols are given at the end of the text.

For calculation of the equilibrium constant (K) of the reactions, activities of the minerals have been assumed to be equal to their mole fraction $(X)\cdot X_{Crd} = (X^{Crd}_{Mg})^2$ where $X_{Mg} = Mg/(Mg+Fe)$; $X_{Pyr} = (X^{Grt}_{Mg})^3$ where $X_{Mg} = Mg/(Mg+Fe+Ca+Mn)$; $X_{Ens} = X^{M1}_{Mg}\cdot X^{M2}_{Mg}$ where X^{M1}_{Mg} is $\{[1-(Al^{VI}+Fe^{+3}+Cr+Ti)]\cdot X_{Mg}\}$ and X^{M2}_{Mg} is $\{[1-(Ca+Mn+Na)]\cdot X_{Mg}\}$, based on formula of orthopyroxene calculated on the basis of six oxygen (Wood and Banno 1973); $X_{Mg} = Mg/(Mg+Fe^{+2})$; $X_{Sp} = X_{Mg}\cdot X^2_{Al}$ where X_{Mg} is the same as in orthopyroxene and $X_{Al} = Al/(Al+Fe^{+3}+Cr+Ti)$; $X_{Spr2:2:1} = X^2_{Mg}\cdot X^4_{Al}\cdot X_{Si}$ where X_{Al} and X_{Mg} are the same as given for spinel and $X_{Si} = Si/2$ from the formula of $Spr_{2:2:1}$ based on 20 oxygen; $X_{Spr7:9:3} = X^7_{Mg}\cdot X^{18}_{Al}$ if Si-content is more than 1.5 from the formula calculated on 20 oxygen basis, if Si-content is less than 1.5, $X_{Spr7:9:3} = X^7_{Mg}\cdot X^{18}_{Al}\cdot X^3_{Si}$ where $X_{Si} = Si/1.5$ from formula calculated on 20 oxygen basis, X_{Mg} and X_{Al} are the same as given for $Spr_{2:2:1}$; $X_{MgTs} = X^{M2}_{Mg}\cdot X^{VI}_{Al}$ or where Al^{VI} is more than Al^{IV}, $X_{MgTs} = X^{M2}_{Mg}\cdot(Al/2)$, X^{M2}_{Mg} is same as given in the calculation of mole fraction of enstatite, Al^{VI} or $Al/2$ is from formula calculated on 6 oxygen basis. The Fe^{+3}-contents of orthopyroxene, spinel and sapphirine (2:2:1 and 7:9:3) are calculated from stoichiometry (see table 2a).

The thermodynamic expressions for the geothermobarometry, derived from the data given in table 1, are arranged in three groups: (**a**) $Spr_{2:2:1}$ equilibria (**b**) $Spr_{7:9:3}$ equilibria and (**c**) MgTs equilibria, groups (a) and (b) include equilibria involving Sp, Qz, Ens, Sil, Pyr and Crd; while group (c) also includes Spr(2:2:1 and 7:9:3) in addition to the minerals given for group (a) and (b).

(a) Sapphirine$_{2:2:1}$ equilibria: P in bars, T in kelvin and $T°C = T$ kelvin -273.15, $R = 1.987\,K^{-1}$.

(1) $2Pyr + 2Qz = 3Ens + 2Sil$

$$P = 1 + \{[T(-5.65 - R\ln K) + 12240]/(0.35277)\}$$

$$K = (a^3_{Ens})/(a^2_{Pyr}).$$

(2) $\mathrm{Ens} + 2\mathrm{Sil} = \mathrm{Spr}_{2:2:1} + 3\mathrm{Qz}$
$T = \{[0.15822(P-1) + 7350]/(7.54 - R\ln K)\}$
$K = (a_{\mathrm{Spr2:2:1}})/(a_{\mathrm{Ens}})$.

(3) $6\mathrm{Pyr} = 2\mathrm{Spr}_{2:2:1} + 7\mathrm{Ens} + 2\mathrm{Sil}$
$P = 1 + \{[T(-1.87 - R\ln K) + 22020]/(1.3748)\}$
$K = (a^2_{\mathrm{Spr2:2:1}} \cdot a^7_{\mathrm{Ens}})/(a^6_{\mathrm{Pyr}})$.

(4) $2\mathrm{Pyr} + 4\mathrm{Sil} = 3\mathrm{Spr}_{2:2:1} + 7\mathrm{Qz}$
$P = 1 + \{[T(16.93 - R\ln K) - 9810]/(0.81788)\}$
$K = (a^3_{\mathrm{Spr2:2:1}})/(a_{\mathrm{Pyr}})^2$.

(5) $2\mathrm{Pyr} = \mathrm{Spr}_{2:2:1} + 2\mathrm{Ens} + \mathrm{Qz}$
$P = 1 + \{[T(1.89 - R\ln K) + 4890]/(0.51099)\}$
$K = (a_{\mathrm{Spr2:2:1}} \cdot a^2_{\mathrm{Ens}})/(a^2_{\mathrm{Pyr}})$.

(6) $\mathrm{Ens} + 2\mathrm{Sil} = 2\mathrm{Sp} + 4\mathrm{Qz}$
$T = \{[0.2538(P-1) + 6360]/(6.15 - R\ln K)\}$
$K = (a^2_{\mathrm{Sp}})/(a_{\mathrm{Ens}})$.

(7) $4\mathrm{Pyr} = 5\mathrm{Ens} + 2\mathrm{Sil} + 2\mathrm{Sp}$
$P = 1 + \{[T(-5.15 - R\ln K) + 18160]/(0.95937)\}$
$K = (a^2_{\mathrm{Sp}} \cdot a^5_{\mathrm{Ens}})/(a^4_{\mathrm{Pyr}})$.

(8) $\mathrm{Pyr} = \mathrm{Qz} + \mathrm{Ens} + \mathrm{Sp}$
$P = 1 + \{[T(0.25 - R\ln K) + 2940]/(0.3033)\}$
$K = (a_{\mathrm{Ens}} \cdot a_{\mathrm{Sp}})/(a_{\mathrm{Pyr}})$.

(9) $\mathrm{Pyr} + 2\mathrm{Sil} = 3\mathrm{Sp} + 5\mathrm{Qz}$
$P = 1 + \{[T(6.40 - R\ln K) - 3420]/(0.5571)\}$
$K = (a^3_{\mathrm{Sp}})/(a_{\mathrm{Pyr}})$.

(10) $\mathrm{Pyr} + \mathrm{Sp} = \mathrm{Spr}_{2:2:1} + \mathrm{Ens}$
$P = 1 + \{[T(1.64 - R\ln K) + 1950]/(0.2077)\}$
$K = (a_{\mathrm{Spr2:2:1}} \cdot a_{\mathrm{Ens}})/(a_{\mathrm{Pyr}} \cdot a_{\mathrm{Sp}})$.

(11) $\mathrm{Ens} + 2\mathrm{Sil} + \mathrm{Qz} = \mathrm{Crd}$
$P = 1 + \{[T(8.40 - R\ln K) - 1220]/(1.0679)\}$
$K = (a_{\mathrm{Crd}})/(a_{\mathrm{Ens}})$.

(12) $\mathrm{Spr}_{2:2:1} + 4\mathrm{Qz} = \mathrm{Crd}$
$P = 1 + \{[T(0.86 - R\ln K) + 6130]/(0.9097)\}$
$K = (a_{\mathrm{Crd}})/(a_{\mathrm{Spr2:2:1}})$.

(13) $4\mathrm{Ens} + 8\mathrm{Sil} = \mathrm{Spr}_{2:2:1} + 3\mathrm{Crd}$
$P = 1 + \{[T(32.74 - R\ln K) - 11010]/(3.3619)\}$
$K = (a_{\mathrm{Spr2:2:1}} \cdot a^3_{\mathrm{Crd}})/(a^4_{\mathrm{Ens}})$.

(14) $2\mathrm{Sp} + 5\mathrm{Qz} = \mathrm{Crd}$
$P = 1 + \{[T(2.25 - R\ln K) + 5140]/(0.8141)\}$
$K = (a_{\mathrm{Crd}})/(a^2_{\mathrm{Sp}})$.

(15) $\mathrm{Pyr} + 2\mathrm{Sil} = \mathrm{Sp} + \mathrm{Crd}$
$P = 1 + \{[T(8.65 - R\ln K) + 1720]/(1.3712)\}$
$K = (a_{\mathrm{Sp}} \cdot a_{\mathrm{Crd}})/(a_{\mathrm{Pyr}})$.

(16) $5\mathrm{Ens} + 10\mathrm{Sil} = 4\mathrm{Crd} + 2\mathrm{Sp}$
$P = 1 + \{[T(39.75 - R\ln K) - 11240]/(4.5253)\}$
$K = (a^4_{\mathrm{Crd}} \cdot a^2_{\mathrm{Sp}})/(a^5_{\mathrm{Ens}})$.

(17) $2\mathrm{Pyr} + 4\mathrm{Sil} + 5\mathrm{Qz} = 3\mathrm{Crd}$
$P = 1 + \{[T(19.55 - R\ln K) + 8580]/(3.5564)\}$
$K = (a^3_{\mathrm{Crd}}/(a^2_{\mathrm{Pyr}})$.

(18) $5\mathrm{Ens} + 6\mathrm{Sil} = 2\mathrm{Crd} + 2\mathrm{Pyr}$
$P = 1 + \{[T(22.45 - R\ln K) - 14680]/(1.783)\}$
$K = (a^2_{\mathrm{Crd}} \cdot a^2_{\mathrm{Pyr}})/(a^5_{\mathrm{Ens}})$.

(19) $2\mathrm{Pyr} + 3\mathrm{Qz} = \mathrm{Crd} + 2\mathrm{Ens}$
$P = 1 + \{[T(2.75 - R\ln K) + 11020]/(1.4206)\}$
$K = (a_{\mathrm{Crd}} \cdot a^2_{\mathrm{Ens}})/(a^2_{\mathrm{Pyr}})$.

(20) $8\mathrm{Pyr} = 3\mathrm{Spr}_{2:2:1} + 8\mathrm{Ens} + \mathrm{Crd}$
$P = 1 + \{[T(8.42 - R\ln K) + 25690]/(2.9536)\}$
$K = (a^3_{\mathrm{Spr2:2:1}} \cdot a^8_{\mathrm{Ens}} \cdot a_{\mathrm{Crd}})/(a^8_{\mathrm{Pyr}})$.

(21) $8\mathrm{Pyr} + 16\mathrm{Sil} = 5\mathrm{Spr}_{2:2:1} + 7\mathrm{Crd}$
$P = 1 + \{[T(73.90 - R\ln K) + 3670]/(9.6773)\}$
$K = (a^5_{\mathrm{Spr2:2:1}} \cdot a^7_{\mathrm{Crd}})/(a^8_{\mathrm{Pyr}})$.

(22) $5\mathrm{Pyr} = 5\mathrm{Ens} + 3\mathrm{Sp} + \mathrm{Crd}$
$P = 1 + \{[T(3.50 - R\ln K) + 19840]/(2.3305)\}$
$K = (a^5_{\mathrm{Ens}} \cdot a^3_{\mathrm{Sp}} \cdot a_{\mathrm{Crd}})/(a^5_{\mathrm{Pyr}})$.

(23) $5\mathrm{Spr}_{2:2:1} = \mathrm{Crd} + 8\mathrm{Sp}$
$P = 1 + \{[T(-4.70 - R\ln K) + 10090]/(1.292)\}$
$K = (a_{\mathrm{Crd}} \cdot a^8_{\mathrm{Sp}})/(a^5_{\mathrm{Spr2:2:1}})$.

(b) Sapphirine$_{7:9:3}$ equilibria:

(24) $7\mathrm{Ens} + 18\mathrm{Sil} = 2\mathrm{Spr}_{7:9:3} + 26\mathrm{Qz}$
$T = \{[1.4173(P-1) + 52960]/(58.87 - R\ln K)\}$
$K = (a^2_{\mathrm{Spr7:9:3}})/(a^7_{\mathrm{Ens}})$.

(25) $7\mathrm{Pyr} + 20\mathrm{Sil} = 3\mathrm{Spr}_{7:9:3} + 32\mathrm{Qz}$
$P = 1 + \{[T(68.53 - R\ln K) - 36600]/(3.3604)\}$
$K = (a^3_{\mathrm{Spr7:9:3}})/(a_{\mathrm{Pyr}})^7$.

(26) $6.5\mathrm{Pyr} = 0.5\mathrm{Spr}_{7:9:3} + 8\mathrm{Ens} + 2\mathrm{Sil}$
$P = 1 + \{[T(-3.645 - R\ln K) + 26540]/(1.5008)\}$
$K = (a^{0.5}_{\mathrm{Spr7:9:3}} \cdot a^8_{\mathrm{Ens}})/(a^{6.5}_{\mathrm{Pyr}})$.

(27) $9\mathrm{Pyr} = \mathrm{Spr}_{7:9:3} + 10\mathrm{Ens} + 4\mathrm{Qz}$
$P = 1 + \{[T(4.01 - R\ln K) + 28600]/(2.2961)\}$
$K = (a_{\mathrm{Spr7:9:3}} \cdot a^{10}_{\mathrm{Ens}})/(a^9_{\mathrm{Pyr}})$.

(28) $\mathrm{Pyr} + \mathrm{Spr}_{7:9:3} = 10\mathrm{Sp} + 6\mathrm{Qz}$
$P = 1 + \{[T(-1.51 - R\ln K) + 800]/(0.7369)\}$
$K = (a^{10}_{\mathrm{Sp}}/(a_{\mathrm{Spr7:9:3}} \cdot a_{\mathrm{Pyr}})$.

(29) $5\mathrm{Pyr} + 4\mathrm{Sp} = 6\mathrm{Ens} + \mathrm{Spr}_{7:9:3}$
$P = 1 + \{[T(3.01 - R\ln K) + 16840]/(1.0829)\}$
$K = (a^6_{\mathrm{Ens}} \cdot a_{\mathrm{Spr7:9:3}})/(a^5_{\mathrm{Pyr}} \cdot a^4_{\mathrm{Sp}})$.

(30) $3.3\mathrm{Ens} + 7\mathrm{Sil} = 2.6\mathrm{Crd} + 0.2\mathrm{Spr}_{7:9:3}$
$P = 1 + \{[T(27.727 - R\ln K) - 8468]/(2.9182)\}$
$K = (a^{2.6}_{\mathrm{Crd}} \cdot a^{0.2}_{\mathrm{Spr7:9:3}})/(a^{3.3}_{\mathrm{Ens}})$.

(31) $2\mathrm{Spr}_{7:9:3} + 33\mathrm{Qz} = 7\mathrm{Crd} + 4\mathrm{Sil}$
$P = 1 + \{[T(-0.07 - R\ln K) + 44420]/(6.0578)\}$
$K = (a^7_{\mathrm{Crd}})/(a^2_{\mathrm{Spr7:9:3}})$.

(32) $2\mathrm{Ens} + 2\mathrm{Spr}_{7:9:3} + 35\mathrm{Qz} = 9\mathrm{Crd}$
$P = 1 + \{[T(16.73 - R\ln K) + 41980]/(8.1936)\}$
$K = (a^9_{\mathrm{Crd}})/(a^2_{\mathrm{Spr7:9:3}} \cdot a^2_{\mathrm{Ens}})$.

(33) $3.5\text{Pyr} = 3.8\text{Ens} + 0.3\text{Spr}_{7:9:3} + 0.4\text{Crd}$
$P = 1 + \{[T(2.303 - R\ln K) + 12988]/(1.2571)\}$
$K = (a_{\text{Ens}}^{3.8} \cdot a_{\text{Crd}}^{0.4} \cdot a_{\text{Spr7:9:3}}^{0.3})/(a_{\text{Pyr}}^{3.5})$.

(34) $3.3\text{Pyr} + 7.6\text{Sil} = 0.5\text{Spr}_{7:9:3} + 3.2\text{Crd}$
$P = 1 + \{[T(32.275 - R\ln K) + 3052]/(4.3536)\}$
$K = (a_{\text{Spr7:9:3}}^{0.5} \cdot a_{\text{Crd}}^{3.2})/(a_{\text{Pyr}}^{3.3})$.

(35) $\text{Pyr} + \text{Spr}_{7:9:3} + 19\text{Qz} = 5\text{Crd}$
$P = 1 + \{[T(9.74 - R\ln K) + 26500]/(4.8071)\}$
$K = (a_{\text{Crd}}^{5})/(a_{\text{Spr7:9:3}} \cdot a_{\text{Pyr}})$.

(36) $\text{Spr}_{7:9:3} + \text{Ens} = \text{Crd} + 7\text{Sp}$
$P = 1 + \{[T(0.49 - R\ln K) + 3000]/(1.2476)\}$
$K = (a_{\text{Sp}}^{7} \cdot a_{\text{Crd}})/(a_{\text{Spr7:9:3}} \cdot a_{\text{Ens}})$.

(37) $0.5\text{Pyr} + 0.5\text{Spr}_{7:9:3} = 0.6\text{Crd} + 3.8\text{Sp}$
$P = 1 + \{[T(0.595 - R\ln K) + 3484]/(0.8569)\}$
$K = (a_{\text{Crd}}^{0.6} \cdot a_{\text{Sp}}^{3.8})/(a_{\text{Pyr}}^{0.5} \cdot a_{\text{Spr7:9:3}}^{0.5})$.

(38) $5\text{Spr}_{7:9:3} = 33\text{Sp} + 10\text{Sil} + \text{Crd}$
$P = 1 + \{[T(-37.3 - R\ln K) + 26240]/(1.7127)\}$
$K = (a_{\text{Sp}}^{33} \cdot a_{\text{Crd}})/(a_{\text{Spr7:9:3}}^{5})$.

(c) Mg-tschermak equilibria:

(39) $\text{Ens} + 2\text{Sil} = 2\text{MgTs} + 2\text{Qz}$
$T = \{[0.0588(P - 1) + 17360]/(9.03 - R\ln K)\}$
$K = (a_{\text{MgTs}}^{2})/(a_{\text{Ens}})$.

(40) $\text{Spr}_{2:2:1} + \text{Qz} = 2\text{MgTs}$
$T = \{[-0.09943(P - 1) + 10010]/(1.47 - R\ln K)\}$
$K = (a_{\text{MgTs}}^{2})/(a_{\text{Spr2:2:1}})$.

(41) $\text{Ens} + 2\text{Spr}_{2:2:1} + 2\text{Sil} = 6\text{MgTs}$
$T = \{[-0.1401(P - 1) + 37380]/(11.95 - R\ln K)\}$
$K = (a_{\text{MgTs}}^{6})/(a_{\text{Ens}} \cdot a_{\text{Spr2:2:1}}^{2})$.

(42) $\text{Sp} + \text{Qz} = \text{MgTs}$
$T = \{[-0.0975(P - 1) + 5500]/(1.43 - R\ln K)\}$
$K = (a_{\text{MgTs}})/(a_{\text{Sp}})$.

(43) $\text{Ens} + 2\text{Sil} + 2\text{Sp} = 4\text{MgTs}$
$T = \{[-0.1362(P - 1) + 28360]/(11.87 - R\ln K)\}$
$K = (a_{\text{MgTs}}^{4})/(a_{\text{Ens}} \cdot a_{\text{Sp}}^{2})$.

(44) $\text{Spr}_{2:2:1} = \text{Sp} + \text{MgTs}$
$T = \{[-0.0019(P - 1) + 4510]/(0.04 - R\ln K)\}$
$K = (a_{\text{Sp}} \cdot a_{\text{MgTs}})/(a_{\text{Spr2:2:1}})$.

(45) $\text{Pyr} = \text{Ens} + \text{MgTs}$
$P = 1 + \{[T(1.68 - R\ln K) - 2560]/(0.20578)\}$
$K = (a_{\text{Ens}} \cdot a_{\text{MgTs}})/(a_{\text{Pyr}})$.

(46) $\text{Pyr} + 2\text{Sil} = 3\text{MgTs} + 2\text{Qz}$
$T = \{[0.2646(P - 1) + 19920]/(10.69 - R\ln K)\}$
$K = (a_{\text{MgTs}}^{3})/(a_{\text{Pyr}})$.

(47) $\text{Pyr} + 2\text{Sil} + 2\text{Sp} = 5\text{MgTs}$
$T = \{[0.0695(P - 1) + 30920]/(13.55 - R\ln K)\}$
$K = (a_{\text{MgTs}}^{5})/(a_{\text{Pyr}} \cdot a_{\text{Sp}}^{2})$.

(48) $\text{Pyr} + 2\text{Spr}_{2:2:1}2\text{Sil} = 7\text{MgTs}$
$T = \{[0.0657(P - 1) + 39940]/(13.63 - R\ln K)\}$
$K = (a_{\text{MgTs}}^{7})/(a_{\text{Pyr}} \cdot a_{\text{Spr2:2:1}}^{2})$.

(49) $8\text{MgTs} = 3\text{Spr}_{2:2:1} + \text{Crd}$
$P = 1 + \{[T(-5.02 - R\ln K) + 46170]/(1.3074)\}$
$K = (a_{\text{Spr2:2:1}}^{3} \cdot a_{\text{Crd}})/(a_{\text{MgTs}}^{8})$.

(50) $2\text{MgTs} + 3\text{Qz} = \text{Crd}$
$P = 1 + \{[T(-0.61 - R\ln K) + 16140]/(1.0091)\}$
$K = (a_{\text{Crd}})/(a_{\text{MgTs}}^{2})$.

(51) $3\text{Ens} + 6\text{Sil} = 2\text{MgTs} + 2\text{Crd}$
$P = 1 + \{[T(25.81 - R\ln K) - 19800]/(2.1945)\}$
$K = (a_{\text{MgTs}}^{2} \cdot a_{\text{Crd}}^{2})/(a_{\text{Ens}}^{3})$.

(52) $5\text{MgTs} = 3\text{Sp} + \text{Crd}$
$P = 1 + \{[T(-4.90 - R\ln K) + 32640]/(1.3016)\}$
$K = (a_{\text{Sp}}^{3} \cdot a_{\text{Crd}})/(a_{\text{MgTs}}^{5})$.

(53) $3\text{Pyr} + 6\text{Sil} = 5\text{MgTs} + 2\text{Crd}$
$P = 1 + \{[T(30.85 - R\ln K) - 27480]/(2.8119)\}$
$K = (a_{\text{MgTs}}^{5} \cdot a_{\text{Crd}}^{2})/(a_{\text{Pyr}}^{3})$.

(54) $\text{Spr}_{7:9:3} + 6\text{Qz} = 7\text{MgTs} + 2\text{Sil}$
$T = \{[-0.5029(P - 1) + 34280]/(2.10 - R\ln K)\}$
$K = (a_{\text{MgTs}}^{7})/(a_{\text{Spr7:9:3}})$.

(55) $\text{Spr}_{7:9:3} + \text{Ens} + 4\text{Qz} = 9\text{MgTs}$
$T = \{[-0.4441(P - 1) + 51640]/(11.11 - R\ln K)\}$
$K = (a_{\text{MgTs}}^{9})/(a_{\text{Ens}} \cdot a_{\text{Spr7:9:3}})$.

(56) $\text{Spr}_{7:9:3} + 3\text{Ens} + 4\text{Sil} = 13\text{MgTs}$
$T = \{[-0.3265(P - 1) + 86360]/(29.13 - R\ln K)\}$
$K = (a_{\text{MgTs}}^{13})/(a_{\text{Ens}}^{3} \cdot a_{\text{Spr7:9:3}})$.

(57) $\text{Ens} + \text{Spr}_{7:9:3} = 5\text{MgTs} + 4\text{Sp}$
$T = \{[-0.054(P - 1) + 29640]/(5.39 - R\ln K)\}$
$K = (a_{\text{MgTs}}^{5} \cdot a_{\text{Sp}}^{4})/(a_{\text{Ens}} \cdot a_{\text{Spr7:9:3}})$.

(58) $3\text{Pyr} + 4\text{Sil} + \text{Spr}_{7:9:3} = 16\text{MgTs}$
$T = \{[0.2909(P - 1) + 94040]/(34.17 - R\ln K)\}$
$K = (a_{\text{MgTs}}^{16})/(a_{\text{Pyr}}^{3} \cdot a_{\text{Spr7:9:3}})$.

(59) $\text{Pyr} + \text{Spr}_{7:9:3} = 6\text{MgTs} + 4\text{Sp}$
$T = \{[0.1518(P - 1) + 32200]/(7.07 - R\ln K)\}$
$K = (a_{\text{MgTs}}^{6} \cdot a_{\text{Sp}}^{4})/(a_{\text{Pyr}} a_{\text{Spr7:9:3}})$.

(60) $3.5\text{MgTs} = 0.3\text{Ens} + 0.3\text{Spr}_{7:9:3} + 0.4\text{Crd}$
$P = 1 + \{[T(-3.577 - R\ln K) + 21948]/(0.5369)\}$
$K = (a_{\text{Crd}}^{0.4} \cdot a_{\text{Spr7:9:3}}^{0.3} \cdot a_{\text{Ens}}^{0.3})/(a_{\text{MgTs}}^{3.5})$.

(61) $11\text{MgTs} + 2\text{Sil} = \text{Spr}_{7:9:3} + 2\text{Crd}$
$P = 1 + \{[T(-3.32 - R\ln K) + 66560]/(2.521)\}$
$K = (a_{\text{Crd}}^{2} \cdot a_{\text{Spr7:9:3}})/(a_{\text{MgTs}}^{11})$.

(62) $\text{Spr}_{7:9:3} + 4\text{Qz} + \text{Pyr} = 10\text{MgTs}$
$T = \{[-0.2383(P - 1) + 54200]/(12.79 - R\ln K)\}$
$K = (a_{\text{MgTs}}^{10})/(a_{\text{Pyr}} \cdot a_{\text{Spr7:9:3}})$.

(63) $3.8\text{MgTs} = 0.3\text{Spr}_{7:9:3} + 0.4\text{Crd} + 0.3\text{Pyr}$
$P = 1 + \{[T(-4.081 - R\ln K) + 22716]/(0.4751)\}$
$K = (a_{\text{Crd}}^{0.4} \cdot a_{\text{Spr7:9:3}}^{0.3} \cdot a_{\text{Pyr}}^{0.3})/(a_{\text{MgTs}}^{3.8})$.

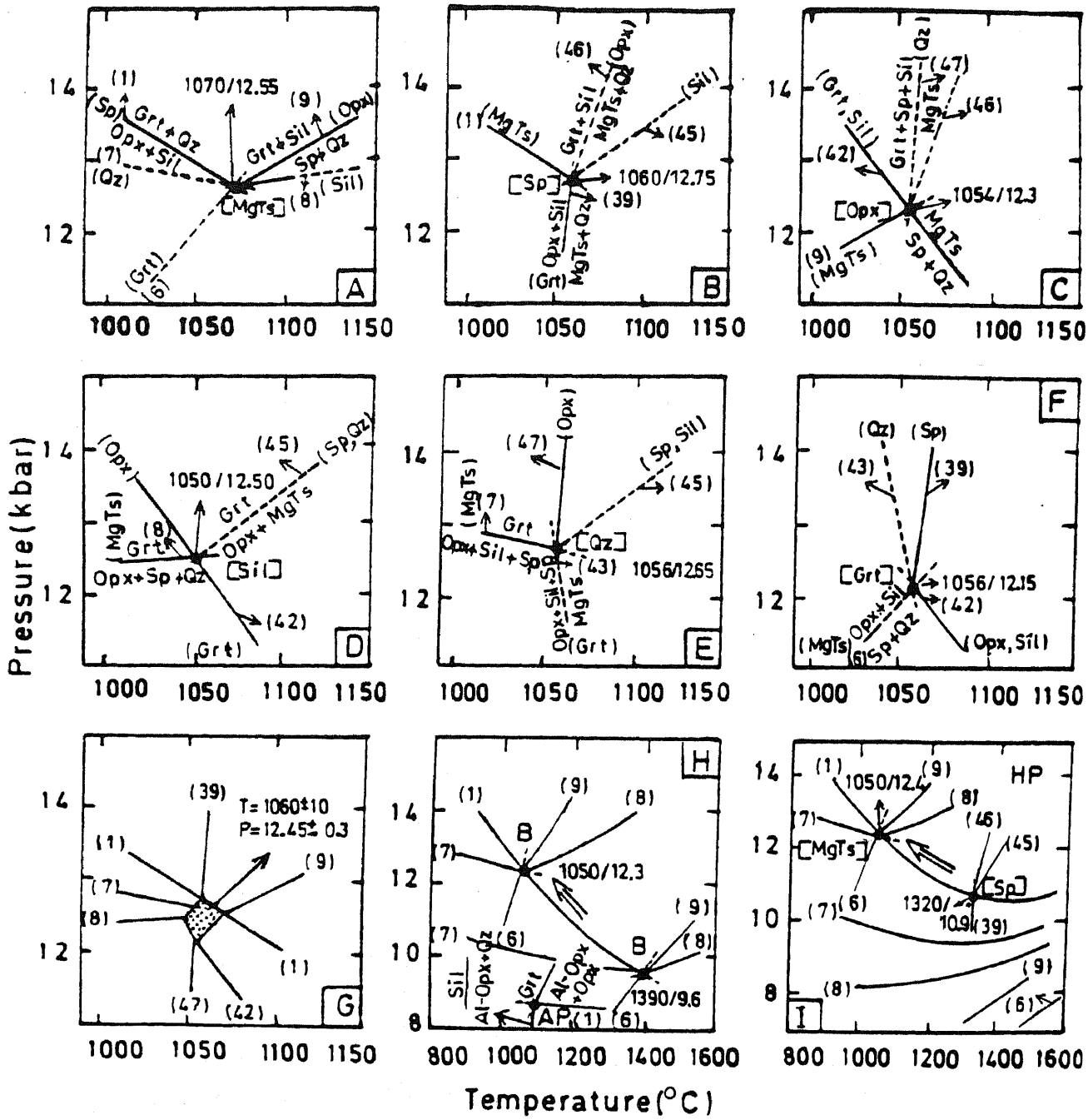

Figure 4. The diagrams (A–G) show the method of estimating P-T simultaneously through intersections of independent mineral equilibria. The method has been used to estimate P-T of Spr-Sp granulites of Eastern Ghats and Enderby Land (figures 5, 6 and 7). The mineral compositions are from experimental run products of sample no. T 3190 at 1050 ± 10°C and 12 ± 0.5 kbar of the equilibrium assemblages containing Grt, Sp, Opx, Sil and Qz in ZnFMAS system (Nichols *et al* 1992). P is in kbar and T in °C. Numbers in the parentheses are equation numbers of the mineral equilibria calibrated for geothermobarometry in this study. Solid curves represent independent mineral equilibria. (G)–stippled area represent P-T estimate from plot of intersections of independent mineral equilibria shown in (A), (B), (C), (D), (E) and (F). The maximum deviation in estimated P-T by this method is shown by the sign $\pm$. The P-T obtained from the calibrations of this study is in good agreement with those of the experimental P-T. (H)–P-T estimate of the same experimental run product sample from 'TWQ' of Berman (1988-B). The number in the parentheses refer to reactions given in equation numbers of the present study. The P-T estimate of 1390°C/9.6 kbar is considerably different compared to the experiment at 1050°C/12 kbar of Nichols *et al* (1992). Arrow shows the shift in P-T estimate from 'TWQ' when γ_{Sp} is assumed to be 0.656. AP–Same with P-T estimate from the calibrations of Aranovich and Podlesskii (1989). Al-Opx–Fictive $AlAlO_3Opx$. Note significant lower pressure estimate compared to the experimental P-T. (I) same as (H) with P-T estimates of the [MgTs] and [Sp] mineral equilibria obtained from 'THERMOCALC' of Holland and Powell (1990-HP). (39), (45) and (46) are MgTs involving reactions given in the corresponding equations of the present study. The curves of the [MgTs] mineral equilibria do not intersect. Arrow shows the shift of P-T estimate of [MgTs] corresponding to those of the experimental P-T when γ_{Sp} is assumed to be 0.626. See text for details and discussion.

The method of estimating P-T simultaneously through intersections of independent mineral equilibria, which have been used for the Spr-Sp granulites of the Eastern Ghats and Enderby Land (figures 5, 6 and 7), is explained in figures 4A to 4G. The experimental run sample no. T 3190 in the ZnFMAS system containing equilibrium assemblage Grt, Sp, Opx, Sil and Qz at 1050 ± 10°C and 12 ± 0.5 kbar (Nichols *et al* 1992) has been used to estimate the P-T by this method. This assemblage, in addition to the other minerals, also includes MgTs. Because of compositional colinearity of Sp-Qz-MgTs and Ens-Pyr-MgTs in the MAS system (see figure 1A, inset upper left), the maximum number of reactions will be 11, 9 non-degenerate univariant reactions involving 4 minerals and 2 degenerate reactions in which 3 minerals participate. There will be 6 invariant points and a maximum of 5 reactions radiating from each of these points, out of which 2 will be linearly independent reactions ($C_p = 5$, $C_s = 3$ and $n_r = 2$, see above). Ideal mixing of Fe-Mg in Grt and Sp and non-ideal regular solution mixing of Zn-Fe and Zn-Mg of Nichols *et al* (1992) have been assumed. The P-T estimate of 1060 ± 10°C/12.45 ± 0.3 kbar from 2 linearly independent reactions from each invariant point define a narrow field (figure 4G), which is consistent with those of the experiments. Similar estimate of P-T from 'TWQ' Berman (1988), Aranovich and Podlesskii (1989) and 'THERMOCALC' Holland and Powell (1990) are also shown in figures 4H and 4I. The estimated P-T deviate significantly from those of the experiments (see above for the discussion and figures 4H and 4I).

5. Application of the geothermobarometers to the sapphirine-spinel granulites of Eastern Ghats and Enderby Land

The P-T conditions of the granulite facies metamorphism of the Spr-Sp granulites have been estimated simultaneously through the intersections of the independent mineral equilibria, with steep and gentle $\mathrm{d}P/\mathrm{d}T$ slopes, applicable to the mineral assemblages (figures 5, 6 and 7). The minerals present in the coronas and other reaction textures in these granulites may or may not be in chemical equilibrium. The coexisting minerals are in chemical equilibrium if the distribution coefficient (K_D) of the minerals in the net transfer reactions is systematic. This will be reflected by a narrow P-T range of intersections of several mineral equilibria assuming that the internally consistent thermodynamic dataset (table 1) is reasonably good. It will be demonstrated below that this is satisfied for most of the reaction textures and coronas which suggests that at least local or mosaic chemical equilibrium has been attained during the formation of these textures, and thus these geothermobarometers, based on equilibrium thermodynamics, can be used to estimate the P-T conditions of metamorphism. For the cordierite-involving mineral equilibria, the P-T estimates are for the condition $P_{H_2O} = 0$. The approximation of the fluid-absent or fluid-deficient condition is in agreement with (i) the common presence of symplectites, coronas and other reaction textures formed during decompression, and coronas developed during isobaric cooling from the thermal-peak by the [Crd] reactions (Ellis 1980; Droop and Bucher-Nurminen 1984; Lal *et al* 1987; Aranovich and Podlesskii 1989; Harley *et al* 1990) and (ii) experiments on dehydration melting in the KFMASH system (Carrington and Harley 1995b) where Crd is undersaturated in H_2O with respect to the coexisting melt phase (see figure 2I).

5.1 *Eastern Ghats (Visakhapatnam district)*

Paderu: This is a classic area where coronas and other reaction textures are well preserved in the Spr-Sp granulites (Lal *et al* 1987) indicating retrograde P-T-t trajectory passing through [Crd] to [Spr] invariant points of the FMAS grid of high fO_2 (figure 1B) of Hensen (1986). Further textures documenting P-T conditions near the (Grt) and (Spr) from the [Sp] invariant point of the FMAS P-T grid of low fO_2 (figure 1A) of Hensen (1986) have also been reported by Lal *et al* (1987). They estimated P-T conditions of 900 ± 60°C/6.5 ± 0.7 kbar (core) to 760 ± 50°C/5 ± 0.6 kbar (rim) from the different calibrations of geothermobarometry, applicable to the Spr-Sp and two pyroxene basic granulites and garnetiferous charnockites, suggesting a decompressive retrograde trajectory. Microprobe analyses of the coexisting minerals from seven Spr-Sp granulites, used to estimate P-T conditions from the calibrations of this study, are given in table 2.

The sample numbers 321 and H-1 contain Grt, Opx, Sill, Qz, Spr, Sp and symplectites of Opx-Kf-Qz ± Sil considered to be a pseudomorph after osumilite. Spr and Sp are in textural equilibrium with Qz and are also successively partially rimmed by second generation of Sil and Opx. The P-T estimates from the compositions of Grt (core), Opx (core), and Sp and Spr in grain contact with Qz (table 2a), derived-from the geothermobarometers of the [Crd] equilibria calibrated in this study are 900 ± 20°C/8.3 ± 0.3 kbar and 905 ± 15°C/8.2 ± 0.2 kbar respectively. The P-T estimated from the rim compositions of the minerals in the coronas are 818 ± 12°C/7.8 ± 0.25 (sample no. 321) and 840 ± 12°C/7.85 ± 0.2 kbar (sample no. H-1) suggesting isobaric cooling from the thermal peak of metamorphism (figures 5A and 5B). In one sample (no. 303, analyses of minerals given in Lal *et al* 1987) coarse Opx contains 10.4 wt% of Al_2O_3 in the core and inclusions of Spr and Sp are present in Opx. Coarse Sil and Qz along with the osumilite

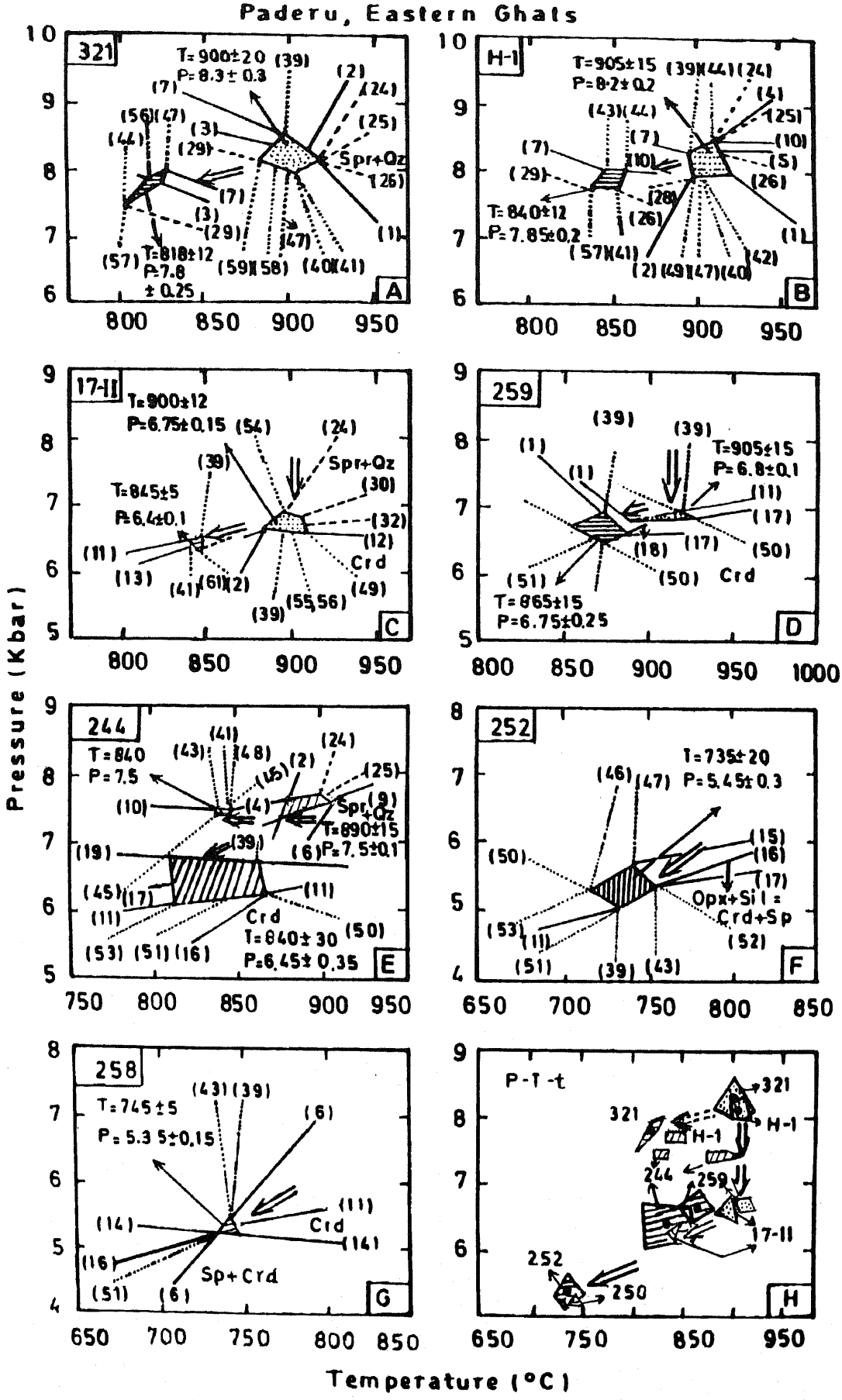
Paderu, Eastern Ghats
321
T=900±20
P=8.3±0.3
Spr+Qz
T=818±12
P=7.8
±0.25
A
H-1
T=905±15
P=8·2±0·2
T=840±12
P=7.85±0.2
B
17-II
T=900±12
P=6.75±0.15
Spr+Qz
T=845±5
P=6.4±0.1
Crd
C
259
T=905±15
P=6.8±0.1
Crd
T=865±15
P=6.75±0.25
D
244
T=840
P=7.5
Spr+Qz
T=890±15
P=7.5±0.1
Crd
T=840±30
P=6.45±0.35
E
252
T=735±20
P=5.45±0.3
Opx+Sil=
Crd+Sp
F
258
T=745±5
P=5.35±0.15
Crd
Sp+Crd
G
P-T-t
321
H-1
244
259
7-11
252
250
H
Pressure (Kbar)
Temperature (°C)

Figure 5.

pseudomorph occur in the matrix. The equations (39) and (57) estimate 920°C at 8 kbar. Simple 244 is characterized by the presence of varieties of coronas and other reaction textures, e.g., (a) Sp-Spr-Sil-Grt, and (b) Sp-Sil-Opx, Spr-Sil-Opx, Sp-Spr-Sil-Opx-Grt (minerals in the coronas arranged from core to rim, and the matrix contains Qz, Kf and Opx-Kf-Qz-Crd symplectite presumably a pseudomorph after osumilite). (c) In the matrix Crd rims Grt and Opx. These textures indicate a *P-T* path passing through (Opx) and (Grt) from the [Crd] invariant point to (Sp) from [Spr] invariant point of the high fO_2 FMAS *P-T* grid (figure 1B). The estimates of the *P-T* from geothermobarometers of this study are (a) 890 ± 15°C/7.5 ± 0.1 kbar (b) 840°C/7.5 kbar and (c) 840 ± 30°C/ 6.45 ± 0.35 kbar suggesting isobaric cooling (figure 5E). The sample no. 252 contains Grt, Sp, Opx, Sil, Qz and Crd, while the sample no. 258 contains the above mineral assemblage apart from Grt thus involving [Spr] and (Spr, Grt) mineral equilibria respectively (figure 1B). Crd forms moats on Sp, Grt, Opx and Sil. The *P-T* estimates are 735 ± 20°C/ 5.45 ± 0.3 kbar and 745 ± 5°C/5.35 ± 0.15 kbar respectively (figures 5F and 5G). The prevalence of high fO_2 in the above mentioned samples is evident from the common presence of ilmenite-hematite intergrowth within the coronas and high Fe^{+3}-contents of Spr, Sp and Sil (table 2a). On the other hand, sample nos. 17II (Opx-Sil-Spr-Crd-Qz, and osumilite pseudomorph) and 259 (Opx-Sil-Grt-Crd-Qz and osumilite pseudomorph) contain rutile, ilmenite, and Fe^{+3} contents of Spr and Sil are low, suggesting low fO_2 conditions. 17 II contains Spr-Sil-Opx, Spr-Sil-Crd coronas in the matrix of Qz, and symplectite of Spr+Crd separating Opx from Sil, indicating *P-T* conditions near the (Grt), [Sp] of the low fO_2 FMAS grid (figure 1A). The *P-T* estimates are (a) core- 900 ± 12°C/6.75 ± 0.15 kbar and (b) coronas- 845 ± 5°C/6.4 ± 0.1 kbar (figure 5C). Sample 259 shows reaction textures, e.g., rims of Crd on Opx, Grt and Sil, suggesting *P-T* near the (Spr) [Sp] (figure 1A). The *P-T* estimates are, core- 905 ± 15°C/ 6.85 ± 0.15 kbar and rim- 865 ± 15°C/6.75 ± 0.25 kbar (figure 5D). The *P-T-t* retrograde trajectory based on the above mentioned samples is shown in figure 5H, e.g., near thermal peak at 900°C/8.3 kbar, isothermal decompression from 900°C/6.85 kbar and decompression at 740°C/5.4 kbar. Isobaric cooling from the thermal peak and also after the isothermal decompression to temperature range 820–865°C is indicated from the *P-T* estimates of the different coronas.

Anantgiri: Sengupta *et al* (1990) reported two types of Spr granulites containing Opx, Spr, Sil, Sp, Qz and Crd (rock type 1, sample no. L-1) and Grt, Opx, Spr, Sil, Qz and Crd (rock type 2, sample no. L-2). Spr and Sp do not occur in grain contact with Qz. They inferred the reaction Crd = Spr + Qz from the textural relations in the rock type 1 and the retrograde reaction Spr + Qz = Opx + Sil and Opx + Sil + Qz = Crd in the rock types 1 and 2. On the basis of the reaction textures and geothermobarometry they proposed an anticlockwise path passing from 900°C/ 7 kbar, 950°C/8.3 kbar (prograde), followed by isobaric cooling 950–700°C/8.3–7.5 kbar and decompression 700°C/5 kbar. The geothermobarometers of the present study yield *P-T* of 930 ± 35°C/6.2 ± 0.2 kbar for the prograde breakdown of Crd to Spr + Qz (see comments below) and decompression from 865 ± 5°C/ 6.15 ± 0.5 kbar to 825 ± 10°C/5.9 ± 0.1 kbar (rock type 1, figure 6A). While for the rock type 2, the *P-T* estimated for the retrograde decompressive path are 870°C/6.8 kbar to 815 ± 20°C/6.35 ± 0.1 kbar (figure 6B). These are in reasonably good agreement with the *P-T* inferred by them. The isobaric cooling from the thermal peak at 950°C/8.3 kbar could not be calculated from the geothermobarometers of this study because the mineral composition of the rock from which this *P-T* has been estimated by them are not given in their paper. The breakdown of Crd to Spr + Qz has been inferred by them from the presence of inclusions of Crd in Spr. It may be pointed out here that retrograde formation of Crd from Spr + Qz may result in Crd forming moats on Spr. Similarly Qz inclusions in Spr would react to form Crd within Spr (cf. Vernon 1996). Motoyoshi and Hensen (1989) suggested the breakdown of Crd to symplectites of Opx + Spr + Qz along a prograde anticlockwise path in Enderby Land (see below). So far no such convincing texture for the prograde breakdown of Crd has been reported from the Eastern Ghats, and thus the inferred anticlockwise prograde loop deduced by Sengupta *et al* (1990) is debatable.

Figure 5. *P-T* estimates derived from intersection of independent mineral equilibria of the different calibrations for geothermobarometry of this study for the Spr-Sp granulites from Paderu, Eastern Ghats. Sample numbers are mentioned in upper left hand corner of the figures (**A–G**). The numbers in the parentheses correspond to equation numbers given in the text. *P-T* estimates are in kbar and *T*°C respectively. The maximum deviation in the *P-T* estimates from the intersection of independent mineral equilibria is shown by the sign ±. Arrow shows the *P-T* path based on textural relations. Bold lines-$Spr_{2:2:1}$ equilibria (group-a), dashed lines-$Spr_{7:9:3}$ equilibria (group-b) and dotted lines-MgTs equilibria (group-c) given in the text. Stippled and ruled areas represent *P-T* estimate of thermal peak from core compositions of minerals and mineral compositions from coronas or reaction textures respectively. The *P-T* estimates from all the seven samples are plotted in (**H**) along with the inferred *P-T-t* trajectory. See text for details. The microprobe data of coexisting minerals, used for geothermobarometry, are given in table 2.

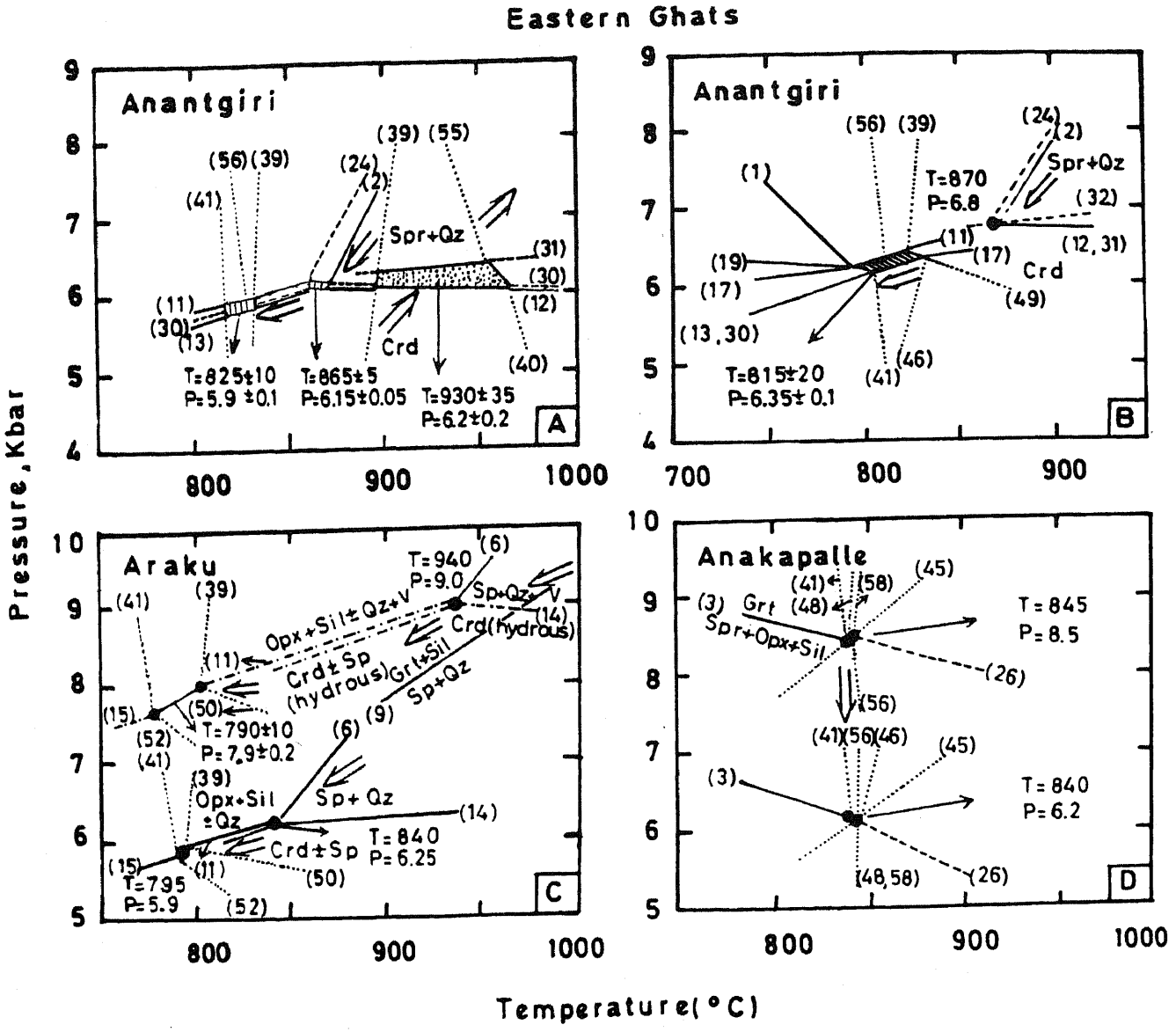

Figure 6. Same as figure 5 for other areas of the Eastern Ghats. P-T paths shown by arrow are those inferred by respective authors. (**A**) and (**B**)–Anantgiri-Spr-Sp granulites samples numbers L-1 and L-2 respectively (Sengupta *et al* 1990). (**C**) Araku–Spr-free Sp granulite, assemblages (i) Sp-Crd-Qz-Opx-Sil and (ii) Grt-Sil-Sp-Qz (Sengupta *et al* 1991). Dashed-dotted curves of reactions (11), (14) and (15) for the assemblage (i) under the condition $P_{H_2O} = P_{Total}$ have been derived from equations of these reactions of the present study along with the equation of hydration of cordierite given in figure 2. P-T curve derived from equation (9) for the assemblage (ii) is also shown. (**D**) Anakapalle–Spr granulite (Dasgupta *et al* 1994). High and low pressure intersections are from massive Spr granulite, sample no. A-1/6 and migmatitic Spr-granulite, sample no. A-7/1 respectively. See text for the details and discussion.

Araku: Sengupta *et al* (1990) reported the assemblages: (i) Sp-Crd-Qz-Opx-Sil and (ii) Sp-Qz-Grt-Sil in the Sp granulite from Araku and proposed the reactions Sp + Crd + Qz = Opx + Sil (Spr, Grt) for (i) and Sp + Qz = Grt + Sil (Spr, Crd, Opx) for (ii). They estimated P-T of 950°C/8.5 kbar which is significantly higher in comparison to those obtained from geothermobarometers of the present study (maximum P-T 840°C/6.25 kbar, figure 6C). High P-T of 940°C/9 kbar is obtained when cordierite is assumed to be saturated in H_2O and/or CO_2 (figure 6C).

Anakapalle: Dasgupta *et al* (1994) reported two types of Spr granulites containing Spr, Grt, Opx, Sil ± Qz, viz., Qz-absent massive type and Qz (minor amounts)-bearing migmatitic type. They found Spr of two generations (a) prograde occurring as inclusions in Grt and (b) retrograde symplectite of Spr, Opx and Sil. The reactions inferred by them are: Spr + Opx + Qz = Grt (Sp, Crd, Sil), Spr + Sil + Opx = Grt (Sp, Crd, Qz) and Grt = Spr + Sil + Opx. They estimated P-T of 900–815°C/8.9–6.1 kbar from geothermobarometry of Spr granulites and associated garnetiferous charnockites and proposed an isothermal

decompression of ≈ 1.5 kbar from the thermal peak of 900°C/8 kbar. The *P-T* obtained (figure 6D) from the geothermobarometry of the present study are 845°C/8.5 kbar (massive Spr granulite, sample no. A-1/6) followed by isothermal decompression at 840°C/6.2 kbar (in migmatitic Spr granulite; sample no. A-7/1) in agreement with Dasgupta *et al* (1994).

Kamineni and Rao (1988) found quartzite containing Sp, Spr, Opx, Grt, Crd and Qz (Sp and Spr occur in grain contact with Qz) from Vizianagaram and inferred *P-T* of 950–1050°C/7–11 kbar, mainly from experimental data in the FMAS system (Hensen and Green 1971, 1972 and 1973). The geothermobarometers of the present calibrations yield intersections spanning a wide range of *P-T* presumably indicating disequilibrium during retrograde path as evident from low MgTs in Opx.

The *P-T-t* trajectory deduced for the Spr-Sp granulites of Eastern Ghats from the present calibrations for geothermobarometry suggests the following: (**a**) A retrograde path from near thermal peak of 900°C/8–8.5 kbar including isothermal decompression to 900–850°C/6.8–6.0 kbar and followed by further decompression to 750°C/5 kbar. (**b**) The anticlockwise (Sengupta *et al* 1990) and clockwise (?) (cf. Lal *et al* 1987) paths joining the retrograde trajectory are debatable as convincing evidence, e.g., breakdown of Crd to form Spr + Opx + Qz symplectite in the anticlockwise case, and Grt containing relics of kyanite and Opx with low Al_2O_3-contents within it, in the clockwise path case, have not yet been reported. (**c**) The inferred *P-T-t* path may also be alternatively explained: (i) as episodes of decompressive heating which may have been short, separated by relatively long period of isobaric cooling during regional decompression (Vernon 1996, figure 13); (ii) multistage alternate episodes of isothermal decompression and isobaric cooling (Sen *et al* 1995), etc. (**d**) The estimate of temperatures of 1000°C or more for the thermal peak is not substantiated from the calibrations of the mineral equilibria involving MgTs of this study. Further Opx should contain 11.5 or more wt% of Al_2O_3 for such high temperature estimates which has not been documented so far (see figure 2G). (**e**) It is premature at this stage to correlate an isobaric cooling from thermal peak of 900°C or more at ≈ 8.5 kbar or more to an earlier event at ≈ 2500 Ma and a decompressive path to a later event at ≈ 1000 Ma.

5.2 *Enderby Land (Archean Napier complex)*

Motoyoshi and Hensen (1989) reported symplectites of Spr + Opx (containing 11.5 wt% Al_2O_3) + Qz along with relics of corroded Crd indicating the reaction Crd = Opx + Spr + Qz (Sp, Grt, Sil) from Mt. Riiser-Larsen, Amundsen Bay. This reaction possibly documents evidence of prograde anticlockwise path. Similar textural relations have been identified from five localities in Enderby Land as mentioned by these authors. They could not estimate *P-T* conditions because none of the existing geothermobarometers are applicable to these granulites. The geothermobarometers of the present study yield *P-T* of 1000°C/7 kbar (figure 7E).

Ellis *et al* (1980) and Ellis (1980) inferred *P-T* of 900–980°C/8–10 kbar mainly from the experimental data of Hensen and Green (1971, 1972 and 1973) in the FMAS system for the Spr, Qz, Grt, Opx (11.33 wt% Al_2O_3 in core), Sil, Crd and osumilite-bearing granulite (sample no. 76283355) from Spot height 945 in Tula Mts. Spr occurs in grain contact of quartz and also in coronas where Spr is successively rimmed by Sil and Grt, or Crd, or Sil-Opx. The reactions inferred by them are: Spr + Qz = Grt+ Crd + Sil (Sp, Opx), Spr + Qz = Crd + Opx + Sil (Sp, Grt) and Spr + Qz = Crd (Sp, Grt, Opx, Sil). The calibrations of the present study yield (**a**) thermal peak 970 ± 20°C/9.1 ± 0.6 kbar, (**b**) isobaric cooling 885 ± 10°C/7.75 ± 0.25 kbar, followed by (**c**) isothermal decompression 880 ± 15°C/6.8 ± 0.25 kbar (figure 7A). The *P-T* estimates of (a) and (b) are in excellent agreement with those inferred by Ellis *et al* (1980) and Ellis (1980).

Grew (1980) reported from Mt. Hardy in the Tula Mts., the assemblage Spr-Opx-Crd-Qz-Sil and inferred the decompressive (Sp, Grt) reaction given above (figure 1A). Crd forms rims on Spr thus isolating Spr from Qz. Grew (1980) estimated *P-T* of 900 ± 30°C/7 ± 1 kbar from a few geothermometers applicable mostly to the associated granulites. The calibrations of this study yield *P-T* of 885 ± 15°C/6.75 ± 0.1 kbar for the Spr granulite (sample no. 2064 E) in excellent agreement with those inferred by him.

Harley (1986) studied in detail a sample (no. 49753) containing the Qz-Opx absent assemblage Grt-Sil-Crd-Sp-Spr from Mt. Sones and inferred the reactions Sp + Crd = Grt + Spr + Sil (Qz, Opx) and Sa + Crd = Grt + Sil (Sp, Qz, Opx). He estimated the *P-T* conditions of 900–950°C/6.5–7.5 kbar from the experimental data of Hensen and Green (1971, 1972, 1973) and the calibration for geobarometry of Waters (1986) for the equilibrium Sp + Crd = Grt + Sil (Sp, Qz, Opx). The garnet-cordierite Fe-Mg geothermometry yields temperatures of 530–680°C. The geothermobarometers of this study estimate *P-T* of ≈ 920 ± 25°C/6.8 ± 0.4 kbar (figure 7C) consistent with those inferred by him. The temperature is approximate only because this is estimated from equations (4), (9) and (25) which involve Qz-bearing mineral equilibria.

Harley *et al* (1990) discussed the metamorphic evolution of Spr-Sp granulites from Forefinger point, SW Enderby Land. They inferred several reactions from textural relations, (**a**) Qz-bearing type (sample no. 4651) – Opx + Sil + Qz = Crd (Spr, Grt, Sp),

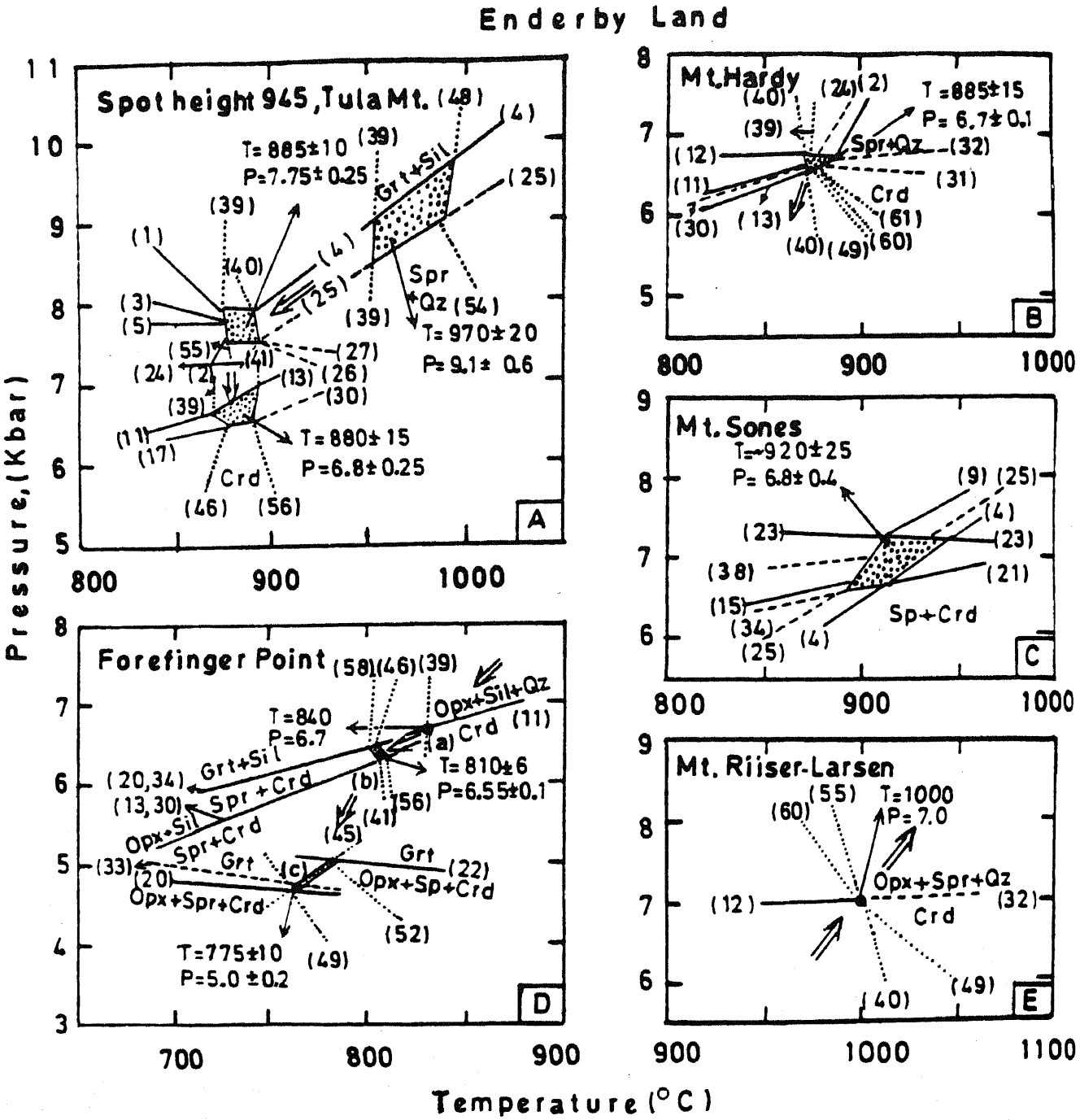

Figure 7. Same as figures 5 and 6 for Spr-Sp granulite from different areas of Enderby Land. (**A**)–Spot height 945, Tula Mts. (Ellis *et al* 1980) sample no. 76283355. (**B**)–Mt. Hardy, Tula Mts. (Grew 1980) sample no. 2064E. (**C**)–Qz-absent Spr-Sp granulite from Mt. Sones (Harley 1986). (**D**) Spr-Sp granulites from Forefinger point, SW Enderby Land (Harley *et al* 1990). With decreasing T from high P, the estimates of P-T from intersection of independent mineral equilibria are those from the sample nos. 4651, 4655 and 4652 respectively. (**E**)–Mt. Riiser-Larsen, Amundsen Bay (Motoyoshi and Hensen 1989), Spr-Opx-Qz-Crd granulite. See text for details and discussion.

(**b**) Qz-absent Sil-bearing type (sample no. 4655) – Opx + Sil = Crd + Spr (Qz, Sp, Grt) and Grt + Sil = Crd + Spr (Qz, Sp, Opx), and (**c**) Qz-Sil absent type (sample no. 4652) – Grt = Sp + Opx + Crd (Qz, Sil, Spr) and Grt = Spr + Opx + Crd (Qz, Sil, Spr). They estimated nearly isothermal decompression > 900°C/10 ± 1.5 kbar to 800–850°C/7–8 kbar and 700–800°C/4.5 ± 1 kbar using a few existing geothermobarometers. The present calibrations yield the following P-T estimates for the mineral equilibria given above: (**a**) 840°C/6.7 kbar, (**b**) 810 ± 6°C/6.55 ± 0.1 kbar and (**c**) 775 ± 10°C/5.0 ± 0.2 kbar (figure 7D) which are in good agreement with those estimated by them for the decompressive path.

It is thus evident that the Spr-Sp granulites of Enderby Land record convincing evidence for anticlockwise prograde and retrograde trajectories deduced from the reaction textures. The *P-T* estimated from the geothermobarometers of this study are: prograde 1000°C/7 kbar to ≈ 1000°C/9 kbar, isobaric cooling ≈ 900°C/8 kbar, isothermal decompression ≈ 900°C/6.5 kbar and decompression up to ≈ 775°C/5 kbar. The entire *P-T-t* trajectory may have involved at least two different major events, a prograde anticlockwise cooling path during ≈ 3000 Ma (Napier complex Archean event) and a later overprinting, reworking and exhumation of these granulites in late Proterozoic Rayner complex metamorphic event at ≈ 1000 Ma resulting in decompressive path (Harley *et al* 1990). However, what happened during the missing 2 Ga is still to be resolved.

The results can be summarized as follows:

- The 63 internally consistent geothermobarometers yield reasonably good estimates of the entire *P-T* conditions and *P-T-t* trajectory of granulite facies metamorphism deduced from the Spr-Sp granulites.
- The maximum deviation from the mean *P-T* estimates given in figures 5, 6 and 7 is practically negligible, in contrast to those obtained from existing geothermobarometers, suggesting that the minerals in the coronas and other reaction textures are at least in local or mosaic chemical-equilibrium on the scale of a thin section. Thus geothermobarometers based on principles of equilibrium thermodynamics can be applied to estimate *P-T* conditions of metamorphism.
- The Spr-Sp granulites which were considered earlier as spectacular museum specimens, act as highly competent 'detectives' that can assemble the scattered fragments or traces of the 'foot prints' of *P-T-t* paths of the metamorphic evolution preserved in varieties of coronas and other reaction textures. The *P-T-t* trajectories deduced would significantly contribute in understanding the geodynamic processes and metamorphic evolution of the deep continental crust during the Precambrian, if supplemented by geophysical and geochronological data.

Acknowledgements

This study is a part of research in the thrust area in metamorphic petrology under the Special Assistance Programme (SAP-DSA) of the University Grants Commission, New Delhi. The computation work has been done on a PC procured under SAP. I thank Prof. S. L. Harley, the reviewer, for his constructive suggestions and criticism.

Abbreviation and symbols

$Spr_{2:2:1}$ and $Spr_{7:9:3}$ Sapphirine end members with molar ratio of $MgO : Al_2O_3 : SiO_2$

Crd	cordierite.	F	FeO
Opx	orthopyroxene.	M	MgO
Pyr	pyrope.	A	Al_2O_3
Sil	sillimanite.	S	SiO_2
Qz	quartz.	K	K_2O
Ens	enstatite.	H	H_2O
Sp	spinel.		
MgTs	Mt-tschermak orthopyroxene.		
Grt	garnet.		
Kf	K-feldspar.		
(a, b ....)	Univariant reactions not involving a, b ... minerals.		
[a, b ....]	Invariant point not involving a, b minerals.		
$\Delta G_{P\text{-}T}$	Gibbs free energy change of reaction at given *P-T*.		
ΔH°_{1000}	Enthalpy change of reaction at 1000 kelvin (K) involving pure phases.		
$\Delta H^\circ f^{oxide}_{1000}$	Molar enthalpy of formation of given mineral with respect to oxides at 1000 (K).		
S°_{1000}	Molar entropy of given mineral at 1000 (K).		
ΔS°_{1000}	Entropy change of reaction at 1000 (K) involving pure phases.		
$V^\circ_{7,1000}$	Molar volume of given mineral at 7 kbar and 1000 (K).		
$\Delta V^\circ_{7,1000}$	Volume change of reaction at 7 kbar and 1000 (K).		
P, T	Pressure in bars and temperature in (K), $T°C = T(K) - 273.15$.		
R	Universal gas constant, 1.987 cal. K^{-1}		
ln	Natural log.		
K	Equilibrium constant.		
K_D	Distribution coefficient.		
fO_2	Oxygen fugacity.		

References

Ackermand D, Seifert F and Schreyer W 1975 Instability of sapphirine at high pressure; *Contrib. Mineral. Petrol.* **50** 79–92

Aranovich L Ya, Podlesskii K K 1983 The cordierite-garnet-sillimanite-quartz equilibrium, experiment and applications; In *Kinetics and equilibrium in mineral reactions*, (ed) S K Saxena (New York: Springer Verlag) 173–198

Aranovich L Ya, Podlesskii K K 1989 Geothermobarometry of high-grade metapelites: simultaneously operating reactions; In *Evolution of metamorphic belts*, (eds) D S Daly, R A Cliff and B W D Yardley (Geol. Soc. Spec. Publ.) **43** 45–61

Audibert N, Hensen B J and Bertrand P 1995 Experimental study of phase relationship involving osumilite in the system K_2O-FeO-MgO-Al_2O_3-SiO_2-H_2O at high pressure and high temperature; *J. Metamorph. Geol.* **13** 331–344

Berman R G 1988 Internally consistent thermodynamic data for minerals in the system Na_2O-K_2O-Cao-Mgo-FeO-Fe_2O_3-Al_2O_3-SiO_2-TiO_2H_2O-CO_2; *J. Petrol.* **29** 445–522

Berman R G and Koziol A M 1991 Ternary excess properties of grossularite-pyrope-almandine garnet and their influence in geothermobarometry; *Am. Mineral.* **76** 1223–1231

Bertrand P, Ellis D J and Green D H 1991 The stability of sapphirine-quartz and hypersthene-sillimanite-quartz assemblages; an experimental investigation in the system FeO-MgO-Al_2O_3-SiO_2 under H_2O and CO_2 conditions; *Contrib. Mineral. Petrol.* **108** 55–71

Bertrand P, Quzegane K H and Kienast J Q 1992 P-T-X relationships in the Precambrian Al-Mg rich granulites from In Quzzal, Hoggar, Algeria; *J. Metamorph. Geol.* **10** 17–31

Bohlen S R, Dollase W A and Wall V J 1986 Calibration and applications of spinel equilibria in the system FeO-Al_2O_3-SiO_2; *J. Petrol.* **27** 1143–1156

Boyd F R and England J L 1959 Pyrope; *Ann. Rept. Dir. Geophys. Lab.* Carnegie Inst., Washington, Year book **58** 83–87

Caporuscio F A and Morse S A 1978 Occurrence of sapphirine plus quartz at Peekskill, New York; *Am. J. Sci.* **278** 1334–1342

Carrington D P and Harley S L 1995a The stability of osumilite in metapelitic granulites; *J. Metamorph. Geol.* **13** 613–625

Carrington D P and Harley S L 1995b Partial melting and phase relations in high-grade metapelites: an experimental petrogenetic grid in KFMASH system; *Contrib. Mineral. Petrol.* **120** 270–291

Charlu T V, Newton R C and Kleppa O J 1975 Enthalpies of solution at 970 K of compounds in the system MgO-Al_2O_3-SiO_2 by high temperature solution calorimetry; *Geoch. Cosm. Acta* **39** 1487–1497

Chatterjee N D and Schreyer W 1972 The reaction enstatite + sillimanite = sapphirine + quartz in the system MgO-Al_2O_3-SiO_2; *Contrib. Mineral. Petrol.* **36** 49–62

Clemens J D, Circone S, Navrotsky A, McMillan P F, Smith B K and Wall V J 1987 Phlogopite: High temperature solution calorimetry, thermodynamic properties, Al-Si and stacking disorder and phase equilibrium; *Geoch. Cosm. Acta* **51** 2569–2578

Dasgupta S, Sanyal S, Sengupta P and Fukuoka M 1994 Petrology of granulites from Anakapalle-Evidence for Proterozoic decompression in the Eastern Ghats, India; *J. Petrol.* **35** 433–459

Droop G T R and Bucher-Nurminen K 1984 Reaction textures and metamorphic evolution of sapphirine-bearing granulites from the Gruf complex Italian Central Alps; *J. Petrol.* **25** 766–803

Ellis D J 1980 Osumilite-sapphirine-quartz granulites from Enderby Land, Antarctica: *P-T* conditions of metamorphism, Implication for garnet-cordierite equilibria and the evolution of the deep crust; *Contrib. Mineral. Petrol.* **74** 201–210

Ellis D J, Sheraton J W, England R N and Dallwitz W B 1980 Osumilite-sapphirine-quartz granulites from Enderby Land, Antarctica: mineral assemblages and reactions; *Contrib. Mineral. Petrol.* **72** 123–143

Gasparik T and Newton R C 1984 The reversed alumina contents of orthopyroxene in equilibrium with spinel and forsterite in the system MgO-Al_2O_3-SiO_2; *Contrib. Mineral. Petrol.* **85** 186–196

Grew E S 1980 Sapphirine + quartz association from Archean rocks in Enderby Land, Antarctica; *Am. Mineral.* **65** 821–836

Harley S L 1986 A. sapphirine-cordierite-garnet-sillimanite granulite from Enderby Land, Antarctica: implication for FMAS petrogenetic grids in the granulite facies; *Contrib. Mineral. Petrol.* **94** 452–460

Harley S L, Hensen B J and Sheraton J W 1990 Two stage decompression in orthopyroxene-sillimanite granulite from Forefinger Point, Enderby Land, Antarctica: implications for the evolution of the Archean complex; *J. Metamorph. Geol.* **8** 591–613

Harris N B W and Holland T J B 1984 The significance of cordierite-hypersthene assemblages from the Beitbridge region of Central Limpopo belt: evidence for rapid decompression in the Archean; *Am. Mineral.* **69** 1036–1049

Hensen B J 1986 Theoretical phase relations involving cordierite and garnet revisited: the influence of oxygen fugacity on the stability of sapphirine and spinel in the system Mg-Fe-Al-Si-O; *Contrib. Mineral. Petrol.* **92** 362–367

Hensen B J and Essene E J 1971 Stability of pyrope-quartz in the system MgO-Al_2O_3-SiO_2; *Contrib. Mineral. Petrol.* **30** 72–83

Hensen B J and Green D H 1971 Experimental study of cordierite and garnet in pelitic compositions at high pressures and temperatures I: compositions with excess alumino-silicates; *Contrib. Mineral. Petrol.* **33** 309–330

Hensen B J and Green D H 1972 Experimental study of cordierite and garnet in pelitic compositions at high pressures and temperatures II: compositions without excess alumino-silicates; *Contrib. Mineral. Petrol.* **35** 331–354

Hensen B J and Green D H 1973 Experimental study of cordierite and garnet in pelitic composition at high pressures and temperatures III: synthesis of experimental data and geological applications; *Contrib. Mineral. Petrol.* **38** 151–166

Holland T J B and Powell R 1990 An enlarged and updated internally consistent thermodynamic data set with uncertainties and correlation in the system K_2O-Na_2O-CaO-MgO-FeO-Fe_2O_3-Al_2O_3-TiO_2-SiO_2-C-H_2-O_2; *J. Metamorph. Geol.* **8** 89–124

Kamineni D C and Rao A T 1988 Sapphirine-bearing quartzite from the Eastern Ghats granulite terrain, Vizianagram, India; *J. Geol.* **96** 209–220

Kleppa O J and Newton R C 1975 The role of solution calorimetry in the study of mineral equilibria; *Fortsch. Mineral.* **52** 3–20

Lal R K 1991 New internally consistent geothermobarometers for the mineral equilibria involving sapphirine, spinel, orthopyroxene, garnet, sillimanite, quartz and cordierite in the MgO-Al_2O_3-SiO_2 system and their application to the granulites; *III Indo-Soviet symposium on 'Experimental mineralogy and petrology'* New Delhi 13–15

Lal R K, Ackermand D, Raith M, Raase P and Seifert F 1984 Sapphirine-bearing assemblages from Kiranur, Southern India: A study of chemographic relationships in the Na_2O-MgO-FeO-Al_2O_3-SiO_2-H_2O system; *N. Jb. Miner. Abh.* **150** 121–152

Lal R K, Ackermand D and Upadhyay H 1987 P-T-X relationship deduced from corona textures in sapphirine-spinel-quartz assemblages from Paderu, Southern India; *J. Petrol.* **28** 1139–1168

Mohan A, Ackermand D and Lal R K 1986 Reaction textures and P-T-X trajectory in sapphirine-spinel-bearing granulites from Ganguvarpatti, Southern India; *N. Jb. Miner. Abh.* **54** 31–49

Motoyoshi Y and Hensen B J 1989 Sapphirine-quartz-orthopyroxene symplectites after cordierite in the Archean: evidence for a counterclockwise *P-T* path?; *Eur. J. Mineral.* **1** 467–471

Newton R C 1972 An experimental determination of the high pressure stability limits of magnesian cordierite under wet and dry conditions; *J. Geol.* **80** 398–420

Newton R C 1987 Thermodynamic analysis of phase equilibria in simple mineral systems; In Thermodynamic modelling of goelogical materials: minerals, fluids and melts (eds) S E Carmichael and H P Eugster; *Rev. Mineral.* **17** 1–33

Newton R C and Perkins D III 1982 Thermodynamic calibration of geobarometers based on the assemblages

garnet-plagioclase-orthopyroxene (clinopyroxene)-quartz; *Am. Mineral.* **67** 203–222

Nichols G T, Berry R F and Green D H 1992 Internally consistent gahnitic spinel-cordierite-garnet equilibria in the FMASHZn system: geothermobarometry and application; *Contrib. Mineral Petrol.* **111** 362–377

Perkins III D 1983 The stability of Mg-rich garnet in the system CaO-MgO-Al_2O_3-SiO_2 at 1000–1300°C and high pressure; *Am. Mineral.* **68** 355–364

Robie R A, Hemingway B S and Fisher J R 1978 Thermodynamic properties of minerals and related substances at 298.15 K and 1 bar (10^5 Pascals) pressure and at higher temperatures; *U.S. Geol. Surv. Bull.* **1452** 456p

Schreyer W and Seifert F 1969 Compatibility relations of the aluminum silicates in the system MgO-Al_2O_3-SiO_2-H_2O and K_2O-MgO-Al_2O_3-SiO_2-H_2O at high pressures; *Am. J. Sci.* **267** 371–388

Seifert F 1974 Stability of sapphirine: A study of the aluminous part of the system MgO-Al_2O_3-SiO_2-H_2O; *J. Geol.* **82** 173–204

Sen S K, Bhattacharya S and Acharya A 1995 A multi-stage pressure-temperature record in the Chilka Lake granulites: the epitome of metamorphic evolution in the Eastern Ghats, India?; *J. Metamorph. Geol.* **13** 287–298

Sengupta P, Dasgupta S, Bhattacharya P K, Fukuoka M, Chakraborti S and Bhowmick S 1990 Petro-tectonic imprints in the sapphirine granulites from Anantgiri, Eastern Ghats mobile belt, India; *J. Petrol.* **31** 971–996

Sengupta P, Karmakar S, Dasgupta S and Fukuoka M 1991 Petrology of spinel granulites from Araku, Eastern Ghats, India, and petrogenetic grid for sapphirine free rock in the system FMAS; *J. Metamorph. Geol.* **9** 451–459

Thompson J B Jr 1982 Reaction space: An algebraic and geometric approach, In: Characterization of metamorphism through mineral equilibria, (ed.) J M Ferry *Rev. Mineral.* **10** 35–52

Vernon R H 1996 Problems with inferring *P-T-t* paths in *L-P* granulite facies rocks; *J. Metamorph. Geol.* **14** 143–153

Waters D J 1986 Metamorphic history of sapphirine-bearing and related magnesian gneisses from Namaqualand, South Africa; *J. Petrol.* **27** 541–565

Wood B J and Banno S 1973 Garnet-orthopyroxene and orthopyroxene-clinopyroxene relationships in simple and complex systems; *Contrib. Mineral. Petrol.* **42** 109–124